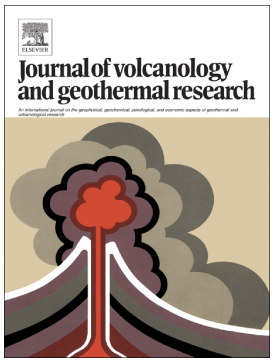

Mobility and emplacement of an ancient, large-volume pyroclastic flow, Ongatiti Ignimbrite, North Island, New Zealand

Elham Yousef Zadeh, Adrian Pittari, David J. Lowe, Martin Danišík

PII: S0377-0273(23)00110-5

DOI: https://doi.org/10.1016/j.jvolgeores.2023.107853

Reference: VOLGEO 107853

To appear in: *Journal of Volcanology and Geothermal Research*

Received date: 20 May 2022

Revised date: 24 June 2023

Accepted date: 27 June 2023

Please cite this article as: E.Y. Zadeh, A. Pittari, D.J. Lowe, et al., Mobility and emplacement of an ancient, large-volume pyroclastic flow, Ongatiti Ignimbrite, North Island, New Zealand, *Journal of Volcanology and Geothermal Research* (2023), https://doi.org/10.1016/j.jvolgeores.2023.107853

Mobility and emplacement of an ancient, large-volume pyroclastic flow, Ongatiti Ignimbrite, North Island, New Zealand

Elham Yousef Zadeh[1], Adrian Pittari[1], David J. Lowe[1], Martin Danišík[2]

[1] School of Science, University of Waikato, Hamilton, New Zealand

[2] John de Laeter Centre, Curtin University, Perth, Australia

Abstract

Pyroclastic flows are the most devastating phenomena of explosive volcanic eruptions. These hazardous fast-moving, hot, concentrated density currents are able to travel several tens of kilometers radially away from their source. Due to an enveloping ash cloud, it is still impossible to directly study pyroclastic flows. However, their deposits (i.e., ignimbrites) provide useful insight into their internal processes of emplacement. This study focuses on the Ongatiti Ignimbrite, which is sourced from Mangakino caldera (i.e., the oldest volcanic centre in the Taupo Volcanic Zone, North Island, New Zealand dated at 1600–950 ka) and offers a unique opportunity to understand the emplacement processes of an ancient and large-volume pyroclastic flow. It is a welded to non-welded, columnar-jointed, cliff-forming deposit, that has been divided into nine facies based on the variation in pumice and lithic clast abundance, and degree of welding.

Our results constrain the minimum deposit volume for the Ongatiti Ignimbrite to ca. 1400 km^3, or 1000 km^3 dense-rock equivalent. Zircon (U-Th)/He data suggest an eruption age of 1.37±0.04 Ma, which is in good agreement with the previous proposed eruption age. The topographic controls on the spatial distribution of the ignimbrite have been determined to understand pyroclastic flow pathways through valleys and over hills. The ignimbrite covered hills up to ~ 900 m (about 650 m above the caldera height) to around 40 km from the Mangakino volcanic center (MVC) and, the pyroclastic flow travelled to beyond 90 km from the vent. The Ongatiti Ignimbrite was a landscape-modifying event that covered at least the western North Island and as far away as Auckland and Wellington.

Key words: Ongatiti Ignimbrite; Mangakino Volcanic Centre; Taupo Volcanic Zone; Pyroclastic flow; Large volume ignimbrite; (U-Th)/He; zircon

1. Introduction

Large-volume pyroclastic flows are hazardous phenomena that bury topography within and beyond calderas and can travel more than 100 km from their source (Cas and Wright, 1987). Explosive super-eruptions, which typically generate large pyroclastic flows, are described as having an ejected magma mass greater than 1 x 10^{15} kg and, for rhyolitic eruptions, estimated to have produced a dense-rock equivalent (DRE) erupted magma volume of more than 450 km^3 (Sparks et al., 2005; Self, 2006; Miller and Wark, 2008; Heron, 2014). Such eruptions are rare, and have never been observed, hence the primary information to understand the physical impacts and destructiveness of supereruption-generated pyroclastic flows is through the examination of their products: large-volume ignimbrites.

The c. 1.3 Ma Ongatiti Ignimbrite is one of the more voluminous rhyolitic ignimbrites in the North Island of New Zealand, and was derived from a super-eruption from a now-buried caldera in the Mangakino Volcanic Centre (e.g., (Martin, 1961; Wilson, 1986; Briggs et al., 1993; Houghton et al., 1995; Wilson et al., 2009). It is typically a welded to non-welded, columnar-jointed ignimbrite that forms prominent bluffs and landscape terraces in the western North Island and is correlated to the distal Oparau tephra (Lowe et al., 2001).

This paper investigates the proximal, medial, and distal emplacement processes, topographic controls and distribution of welding of the Ongatiti Ignimbrite and its distal tephra. The stratigraphic and facies characteristics of the ignimbrite are described and assessed with geographic information system (GIS) data and a digital elevation model (DEM) of the deposit, and a new volume is estimated. New zircon (U-Th)/He ages are presented and discussed with respect to existing eruption ages.

2. Geological Setting

2.1 Mangakino Volcanic Center (MVC)

The NNE-trending Taupo Volcanic Zone (TVZ), central North Island, is approximately 300 km long and 60 km wide and has been active for around two million years (e.g., (Wilson et al., 1995b; Wilson and Rowland, 2016). Rhyolitic volcanism from the TVZ includes at least 34 caldera-forming ignimbrite eruptions and a wide range of minor eruptions from at least eight

rhyolitic centres (Healy, 1964; Houghton et al., 1995; Allan et al., 2008).

An early-TVZ locus of rhyolitic volcanism, situated at the western border of the TVZ, is the 1.6-0.95 Ma Mangakino Volcanic Centre (MVC) (Houghton et al., 1995; Wilson et al., 1984), which was confirmed as a caldera by Rogan (1982) based on a gravity anomaly. The caldera produced >1000 km^3 (DRE) of pyroclastic deposits from multiple explosive eruptions and is now buried beneath younger ignimbrites, lacustrine and fluvial sediments and tephras (Fig. 1a) (Briggs, 1976; Stern, 1979; Rogan, 1982; Briggs et al., 1993; Wilson et al., 2009; Wilson and Rowland, 2016). However, there may be some exposed relief along the southwestern margin as seen in the DEM for the MVC (Fig. 2).

The volcanic succession of the MVC comprises the Pakaumanu Group, which includes four widespread welded, silicic ignimbrites (Ngaroma, Ongatiti, Ahuroa and Rocky Hill ignimbrites), two phreatomagmatic, non-welded, silicic fall and ignimbrite deposits (Unit D and Kidnappers deposits), several poorly exposed silicic and andesitic ignimbrites, and minor lava domes (Wilson, 1986; Briggs et al., 1993; Houghton et al., 1995; Leonard et al., 2010; Pittari et al., 2021). The Ongatiti and Kidnappers ignimbrites are the two most voluminous ignimbrites (>1000 and 1200 km^3 respectively) of the MVC (Houghton et al., 1995; Wilson et al., 1995a; Cooper et al., 2012; Cooper and Wilson, 2014).

Ongatiti Ignimbrite

The Ongatiti Ignimbrite is a widespread, compound, non- to partially welded, vitrophyric pumice- and crystal-rich (plagioclase > quartz > orthopyroxene > hornblende + iron oxides; accessory zircon and apatite), rhyodacitic to rhyolitic ignimbrite with a moderate lithic clast content (e.g., (Martin, 1961; Briggs et al., 1993; Houghton et al., 1995; McCormack et al., 2009; Leonard et al., 2010; Cooper and Wilson, 2014). It is exposed mostly in western areas of the central North Island, and the type section (for Ongatiti, Ahuroa and Rocky Hill ignimbrites) occurs on the southern slopes of Rocky Hill (Lat./Long.: -38.382575, 175.308598) – alongside Ahoroa Road, above the Ongatiti Stream valley (Kear, 1960; Martin, 1961). Isolated exposures occur 75 km northeast of MVC at Tauranga (Briggs et al., 2005), and it is inferred to occur in drill holes at the Waiotapu geothermal field ~60 km to the east (Wilson et al., 2010). Previous estimates of the volume (as deposited material) range from >300 to 1000 km^3 (Wilson, 1986;

Briggs *et al.*, 1993; Houghton *et al.*, 1995). The Ongatiti Ignimbrite is composed of multiple flow units erupted in a series of directional lobes and has previously been divided into a lower highly energetic, pumice-poor facies and an upper less energetic coarse pumice-rich facies (Wilson, 1986; Briggs et al., 1993).

Distal deposits correlated to the Ongatiti Ignimbrite are called the Oparau Tephra (equivalent to member K12 of the Kauroa Ash Formation) in the west of the central North Island (Pain, 1975; Horrocks, 2000; Lowe et al., 2001; Hopkins et al., 2021). Equivalent distal tephra correlated by glass isothermal plateau fission track (ITPFT) dating that occur around Auckland and Wellington, have been referred to as the Ongatiti Tephra (Alloway et al., 2004; Mildenhall and Alloway, 2008). Also, glass chemical compositions of the offshore AT-311 tephra in Ocean Drilling Program (ODP) cores east of the North Island by Alloway *et al.* (2005) indicate a graphical correlation with the Ongatiti Tephra. Mangatewaiti Tephra in Hawke's Bay – a 4-m-thick tephra bed with a crystal-rich base and finely laminated upper part – has a glass-ITPFT age of 1.23 $\pm$ 0.09 Ma and a similar chemistry to the lower nonwelded glass of the Ongatiti Ignimbrite, and has been suggested as a correlative (Shane et al. (1996). The locations of these distal sites are shown in Figure 1b.

3. Methods

This paper combines digital GIS mapping from existing datasets and field confirmation, with selected sites in the field for stratigraphic and facies analysis. Field locations are shown in Figure 3.

Stratigraphic logs were prepared at eight sites located to the north and west of the MVC and at ranging between ~15 (Waipari Gorge) to about 90 (Bryant Home) km from the caldera margin. There were no surface outcrops on the eastern side of the caldera and any possible intra-caldera deposits have been buried. Facies observations in the field included maximum observable thickness and contact relationships, depositional structure (bedforms, grain size grading), grain textural characteristics (lithic and pumice size, sorting and roundness), and lithic, pumice and free crystal types and their abundance. The maximum pumice and lithic clasts sizes were measured as the average of the long axis length of the five largest clasts. Pumice aspect ratios (length x height) for the same five clasts at each observation location were also measured.

Percentage abundances of the pumice and lithics are visual estimates.

The grain size distribution of an ash layer found locally at the Hinuera site was determined by a Malvern Mastersizer at the University of Waikato (see the supplementary file).

Digital GIS data were used to generate two and three-dimensional maps of the distribution of the Ongatiti Ignimbrite. A DEM with a pixel size of 80 m was generated (source data from https://koordinates.com) for the study region and a digital geological map (scale = 1:250,000) in the format of a vector-shape file acquired from GNS Science Geological Map (Heron, 2014) were modified and then used for this study. Additional sources of data, including digital geomorphologic, drainage and boundaries maps, obtained from Land Information New Zealand (LINZ) (http://data.linz.govt.nz), Landcare Research, and Statistics New Zealand and Ollivier and Company (http://www.ollivier.co.nz), have been utilized in the study. Digital datasets were processed using Esri® ArcMap 10.3, and distances and areas were calculated to show the relationship between paleotopography and ignimbrite distribution.

Three samples of the Ongatiti Ignimbrite were collected from the Ongatiti Valley (west of MVC), Hinuera (north of MVC) and Tauranga (northeast of MVC) sites (Fig. 3) for zircon (U-Th)/He dating, to correlate the age spatially around the MVC and also to resolve inconsistencies with the published ages (see Section 4). Zircon crystals were separated from crushed rock samples by standard gravity and magnetic methods and selected under the microscope by hand picking. Zircon (U-Th)/He analyses were conducted at Curtin University, Perth, Australia and followed the procedures described in Danišík et al. (2020). In brief, ^{4}He was extracted at ~1250°C under ultra-high vacuum in an Alphachron I instrument using a diode laser, and its volume was measured by isotope dilution on a QMS 200 Pfeiffer Prisma mass spectrometer. After the He measurements, the crystals were spiked with ^{235}U and ^{230}Th, dissolved in Parr acid digestions vessels, and analyzed by isotope dilution for ^{238}U and ^{232}Th, and by external calibration for ^{147}Sm on an Agilent 5500 ICP-MS. The zircon (U–Th)/He ages were corrected for alpha ejection (Ft-correction) after Farley et al. (1996), whereby homogenous distributions of U, Th, and Sm were assumed for the crystals.

4. Results and interpretation

4.1 Compilation of published ages and new (U-Th)/He data

New zircon (U-Th)/He ages (weighted averages, ± 2s; group IV, Table 1) for the Ongatiti Ignimbrite are 1.31 ± 0.09 Ma at Hinuera, 1.38 ± 0.06 Ma at Tauranga and 1.38 ± 0.05 Ma in the Ongatiti Valley and combination off all data representing a weighted mean age 1.37± 0.04. The full (U-Th)/He data are presented in the supplementary file. These eruption ages are in good agreement with the published geochronological reported for the Ongatiti Ignimbrite summarized in Pittari et al. (2021) and presented in Table 1.

The earliest eruption ages on the proximal ignimbrite were by K/Ar or $^{40}Ar/^{39}Ar$ methods (group I; Table 1). The corrected $^{40}Ar/^{39}Ar$ age on feldspar separates of 1.21 ± 0.04 Ma (plateau age, ±1σ error) reported by Houghton *et al.* (1995), supersedes earlier $^{40}Ar/^{39}Ar$ ages reported in Pringle et al. (1992) and Briggs et al. (1993). An alternative $^{40}Ar/^{39}Ar$ age, also on feldspar separates, of 1.32 ± 0.01 Ma (plateau age, ±1σ error) or 1.34 ± 0.02 Ma (isochron age, ± 1σ error) was reported by Briggs et al. (2005) for a sample near Tauranga. Soengkono et al. (1992) reported a K/Ar age on hornblende separate of 1.25 ± 0.09 Ma. Comparable ages were obtained by glass-ITPFT (1.25 ± 0.12 Ma, Black et al., 1996) and by red thermoluminescence in quartz (1.280 ± 0.165 Ma, Fattahi and Stokes, 2000),

SHRIMP zircon U-Pb crystallization ages (group II, Table 1) have been reported as (all ± 2σ) 1.31 ± 0.03 Ma (Brown and Smith, 2004), 1.29 ± 0.07 Ma (McCormack et al, 2009), or 1.32 ± 0.01 Ma (mean of all zircons) to 1.28 ± 0.02 Ma (zircon rims) (Cooper et al., 2014). Cooper *et al.* (2014) inferred a time delay between the crystallisation of zircon in the magma and the subsequent eruption, the latter assumed to be the $^{40}Ar/^{39}Ar$ age of Houghton et al. (1995). However, they also recognised the possibility that the Houghton *et al.* (1995) age may need revision in light of the $^{40}Ar/^{39}Ar$ age of Briggs *et al.* (2005), which is similar to the zircon crystallization ages.

Distal tephra correlatives (group III, Table 1) have been dated by zircon fission track method (Oparau Tephra/K12, 1.28 ± 0.11 Ma, Lowe et al., 2001; Hopkins et al., 2021), glass-ITPFT (Ongatiti Tephra at Oruarangi, 1.14 ± 0.06 Ma and 1.29 ± 0.14 Ma, Alloway et al., 2004; Tephra AT-62 and AT-63 at the Patiki core site, 1.21 ± 0.08 Ma and 1.18 ± 0.09 Ma, Mildenhall and

Alloway 2008; Mangatewaiiti Tephra, 1.23 ± 0.09 Ma, Shane et al., 1996), $^{40}Ar/^{39}Ar$ method on feldspar (Mangatewaiiti Tephra, 1.24 ± 0.07 Ma, Shane et al., 1996) and by graphical correlation (AT-311 Tephra, 1.202 Ma, Alloway et al., 2005).

4.2 Distribution

A map of the present outcrop distribution of the Ongatiti Ignimbrite in Figure 3. Determining the original distribution of the Ongatiti Ignimbrite has limitations because of erosion of the original ignimbrite sheet and burial by younger deposits, especially on the eastern side of the source caldera where there are no exposed outcrops. Furthermore, the paleotopography prior to ignimbrite emplacement has been modified by ongoing erosion and burial by the Ongatiti ignimbrite sheet and younger pyroclastic deposits.

Our assessment of ignimbrite distribution and volume does not include areas on the eastern side of the MVC where there is no outcrop (except in Tauranga to the northeast), nor of any intracaldera deposit, which is now buried.

Proximal and medial deposits of the Ongatiti Ignimbrite were studied at eight locations and distal deposits at three locations (Fig. 3). The deposit distribution of the ignimbrite was classified into two mapped zones categorized as *'reliable'* and *'expected'*, and a further undefined number of distal deposits that have not counted towards the volume but imply an additional *'possible'* area of distribution. 'Reliable' and 'expected' zones are shown in Figure 4; 'possible' areas are not delineated due to lack of data. The areas that show present-day exposures are classified as 'reliable'; they cover around 1100 km^2, and mainly include proximal and medial deposits. 'Expected' deposits include land that includes the ignimbrite in proximal and medial regions, typically between areas of modern-day exposure, adding a further approximately 6,000 km^2. We assume that the proximal and medial areas were buried by the widespread pyroclastic flow deposit from high elevations to lowlands.

At sites where the equivalent (correlative) distal tephra deposits were studied, we extended our estimation of the areal extent of the Ongatiti Ignimbrite. The extra area covered by distal deposits and the areas between them are defined as the 'possible' zone although for reasons mentioned above this zone was not mapped. The average measured thickness of the deposits in the 'expected' zone is around 3 m, in comparison to the thickness in reliable areas, which is

generally >15 m.

Ongatiti-equivalent distal tephras described around Auckland, Wellington, Hawkes Bay and in Ocean Drilling Project cores (Alloway et al., 2004; Alloway et al., 2005; Mildenhall and Alloway, 2008) allow extension of the Ongatiti deposit to more than 10,000 km^2, but the map distribution in these areas is poorly constrained. This extended area is defined as the 'possible' zone and was not included in our quantitative estimates of the volume. Note, that distal tephras on the west coast (Hauturu, Oparau Creek and Bryant Home localities) have confident mapped areas, were considered part of the 'reliable' zone, and as such were included in the quantitative volume estimate (Fig. 4).

In proximal areas, the ignimbrite covers both hills and valleys and in the latter the greatest thicknesses are observed; also here the deposits lie up to 900 m above sea level (asl), or up to 650 m above the modern topographic surface overlying the caldera (Fig. 5). Medial areas are mostly characterized by valley-filling geometries, which reach elevations of approximately 150–300 m above sea level (asl), comparable to the elevation of the existing caldera topographic surface. The distal equivalents (Oparau Tephra and equivalent K12 unit) were deposited at elevations of <50 m a.s.l. The maps presented here (Figs. 3–5) and the deposits identified during fieldwork also indicate that the ignimbrite extends over 75 km to the NNE and ~90 km to the NW of its caldera source.

The ignimbrite aspect ratio, which uses the aerial distribution and thickness data, was estimated to be between 1:950, based on 'reliable' distribution, and 1:1880 on the 'expected' distribution. Walker (1983) related the aspect ratio to the energy of a pyroclastic flow: low aspect ratio (<1:1000) types are characterized by widespread, thin deposits; and high aspect ratio (>1:1000) deposits are thick and spread locally. The Ongatiti Ignimbrite is a widespread deposit that lies on the boundary between low and high aspect ratio. The original deposit distribution for a low aspect ratio ignimbrite can be evaluated by drawing a single cover area around all of the present-day exposures and calculated areas; however, for high aspect ratio types, drawing multiple envelopes around the exposure is required (Wilson, 1991; Cook et al., 2016). For our calculation we have used the method for low aspect ratio ignimbrite.

4.3 Volume

The estimation of pyroclastic flow deposit volumes is difficult, particularly where the deposits are eroded or only proximal deposits are preserved (Pyle, 1995). The Ongatiti Ignimbrite is highly eroded, proximal and medial outcrops occur predominantly on the western side of the MVC, and there is no evidence for intra-caldera deposits and co-ignimbrite ash fall (Fig. 5). Hence, calculation of the ignimbrite volume is limited only to a minimum estimate.

The method for volume calculation of Wilson (1991), and developed by Cook et al. (2016), was adopted here, which varies in the way dispersal area envelopes are approximated depending on whether the ignimbrite has a high or low aspect ratio. The Ongatiti Ignimbrite, was considered as a low aspect ratio ignimbrite, hence a broad dispersal envelope was approximated over the expected and reliable zones (Fig. 4), and also incorporated the average thicknes of the deposit. First. using the reliable and expected zones within proximal to medial areas and average thickness on the northern and western sides of the MVC, the minimum (loose) deposit volume of the ignimbrite is at least 225 km^3. Second, for the distal deposits that were also mapped as 'reliable' (Oparau Creek, Hauturu, Bryant Home), the minimum volume of the Ongatiti Ignimbrite is at least 15 km^3. Therefore, the total reliable and expected volume for the ignimbrite outflow deposit is at least 240 km^3.

Large eruptions are normally accompanied by a large volume of co-ignimbrite ash-fall deposits (Sparks and Walker, 1977). However, such a deposit associated with the Ongatiti Ignimbrite is not preserved. Furthermore, the intracaldera deposits are now buried. Lipman (1984) observed in western North America calderas that outflow ignimbrites are approximately equal to the volume of intra-caldera deposits. Rose and Chesner (1987) found the relationship between intra-caldera ignimbrite, outflow ignimbrite and co-ignimbrite ash at Toba is around 1000:1000:800 km^3. For the Oruanui Ignimbrite, the calculated relationship was 420:320:430 km^3 (Wilson, 1991). Mason et al. (2004) noted that for both eruptions the ratio of the intra-caldera, outflow, and co-ignimbrite volumes are generally the same. Cook et al. (2016) also suggested a 1:1:1 relationship for the Otowi Member of the Bandelier Tuff in Mexico. Assuming a similar relationship for the Ongatiti Ignimbrite and its possible intra-caldera and co-ignimbrite deposits, we suggest a total minimum deposit volume of approximately 720 km^3.

The Ongatiti Ignimbrite is partially welded in proximal and medial areas and in distal areas it is non-welded. Moon (1989) measured the average density for partially welded Ongatiti Ignimbrite to be 1725 kgm^{-3} and for the non-welded deposit, 1320 kgm^{-3}. These values were used here to calculate the dense rock equivalent volume (DRE), reducing partially welded ignimbrite by a factor of 0.70 (i.e. expected and reliable zones in the proximal-medial areas, Fig. 4) and non-welded ignimbrite by a factor of 0.53 (i.e. reliable zone in the distal sites at Hauturu, Oparau Creek and Bryant Home, Fig. 4). Hence, the minimum DRE volume for the Ongatiti Ignimbrite is estimated to be 512 km^3. However, as mentioned it has been expected that the ignimbrite was emplaced radially around the Mangakino Caldera, and on the western side deposits were eroded or covered by younger ignimbrites. Hence, we can extend the minimum estimation to the eastern side and estimate the minimum deposit volume could be about 1400 km^3 and minimum 1000 km^3 DRE.

As mentioned, flow runout traveling from the source caldera margin to NNE and NW, where there was the least interaction with topography, measured 75 km and 90 km respectively, indicating a mean runout (R) of 82.5 km. Using the relationship between runout distance for concentrated pyroclastic flows and mass discharge rate, Q, of Roche et al. (2021), a mean value for Q of 2 x 10^{11} kgs^{-1} is determined for the Ongatiti Ignimbrite, with a range of possible values between 3 x 10^{10} and 1 x 10^{12} kgs^{-1} from 95% prediction intervals (cf. figs. 4 and 5 of Roche et al., 2021). These values are well within the expected values for a caldera-forming eruption. Additionally, the estimated means for R and Q stated above show strong support for the Ongatiti Ignimbrite bulk volume being >1000km^3 (Fig 6) (see figs. 6a and b of Roche et al., 2021).

4.4 Ignimbrite facies and stratigraphy

The original plateau formed above the Ongatiti Ignimbrite is dissected and, in some areas, the ignimbrite now caps the tops of hills. In proximal areas, the ignimbrite occurs both within valleys and over hills, but in medial and distal areas the deposit characteristics suggest that the pyroclastic flow was channelized through the antecedent valleys.

The ignimbrite is commonly vertically jointed with a joint spacing of 3 to 10 m. Columnar joints with polygonal cross-sections form during cooling and compaction of the ignimbrite, usually perpendicular to the cooling surface (Fisher and Schmincke, 1984; Cas and Wright, 1987;

DeGraff and Aydin, 1987; Aydin and DeGraff, 1988; Moon, 1993) . Columnar joints are commonly vertical in ignimbrites and are usually seen in moderately to highly welded deposits (Fisher and Schmincke, 1984). Moon (1989) classified joint geometry as unjointed, columnar, blocky, and complex. Joint spacing has been classified by Barton (1978) as extremely close (<20 mm), very close (20–60 mm), moderate (200–600 mm), wide (600–2000 mm), very wide (2000–6000 mm) and extremely wide (>6000 mm). In proximal-medial areas, the Ongatiti Ignimbrite has very wide to extremely wide columnar joints, with the only exception at the Peacockes site which is unjointed. Horizontal jointing was also seen at Hinuera and Castle Rock, both approximately in the middle of outcrops. The partially welded to welded nature of the Ongatiti Ignimbrite is consistent with very wide to extremely wide columnar joints (Fisher and Schmincke, 1984). In the following section, the proximal-medial and distal deposits of the Ongatiti Ignimbrite are described separately.

Six different lithofacies are defined here for the Ongatiti Ignimbrite in proximal to medial areas based on pumice and lithic clast size, pumice, lithic and crystal abundances, and degree of welding (Fig. 7a). In section 4.4.2, a further three tephra facies are defined in the distal areas (Fig. 7b).

4.4.1 Proximal-medial ignimbrite facies

Pumice- and lithic-rich facies (PRLR) is a partially welded facies that is also crystal-rich and characterized by large pumice clasts (typically 100 to 450 mm in diameter) comprising 15 to 30% of the bulk ignimbrite and lithic clasts, 7–10% in abundance (Fig. 8a). Pumice clasts occur mostly as four different textural types: vesicular, woody, dense, and rare grey pumice (Fig. 11). Vesicle morphologies are typically spherical or sub-parallel elongate, vary in size from a few millimeters to several centimeters in diameter (maximum vesicle size was measured at Waipari Gorge West at around 15 cm). The pumice aspect ratio is mostly between 2 to 4. Lithic fragments are angular to sub-angular and their maximum size was 60 mm at Waipari Gorge West. Average lithic size and abundance are greater at northern localities (e.g., Hinuera Quarry).

Pumice-rich, lithic-poor facies (PRLP) is a slightly welded to welded facies, rich in pumice and crystals but poor in lithic clasts. The facies is characterized by the abundance (15–25% of the bulk rock) and large maximum size (up to 350 mm) of sub-rounded pumice fragments. They are

mostly vesicular and woody with a cream to white colour. The aspect ratio is usually between 2 to 3.5. Lithic clasts are rare (1–2% of the bulk rock) and they are usually small (maximum size typically 25 mm). This facies is found west and northwest of the MVC (Fig. 8b).

Flattened pumice-rich facies (FPR) occurs as a welded zone with flattened pumice, with a thickness variation from one to 4 m between intervals of PRLR and PRLP facies (Fig. 8c). The maximum pumice aspect ratio is typically 6 and the largest pumice was 400 mm. The zone is classified here as separate facies here due to the welding texture, rather than the abundance and size of components (cf. PRLR, PRLP, PLP). Whilst the abundance of lithic clasts is different (around 5%), the facies is still rich in pumice (cf. PRLR, PRLP).

Pumice- and lithic-poor facies (PPLP) is a slightly to partially welded facies that is poor in both pumice and lithic fragments (Fig. 8d). The percentage of pumice is less than 15% and the maximum size is 100 mm with an aspect ratio of 1.5 to 2. The pumice clasts are mostly vesicular with tiny vesicles and are cream to yellow in colour. Lithic fragments are very rare, about 2% of the bulk rock, with a maximum size of approximately 20 mm. The PPLP facies occurs at the base of exposed sections north of the MVC (i.e., at Hinuera Quarry and Tauranga), and at the top of sections to the north-west (i.e., Waipari Gorge West and Castle Rock).

Pumice-poor, lithic-rich facies (PPLR) occurs as a 10-15 cm thick lithic-rich layer that was recognized only near the lower boundary of the Ongatiti Ignimbrite at Waipari Gorge East. The lithic abundance is >10% and the average lithic size is around 55 mm, comprising mostly angular greywacke and andesite (Fig. 8e). This facies is comparable to the lithic concentration zone (LCZ) at the base of layer 2b in the ignimbrite facies model of Sparks *et al*. (1973).

Fine ash facies (FAL) occurs as two fine ash layers, 10 and 50 mm thick, only recognized locally at the Hinuera section (Fig. 8f). Their median grain sizes are approximately 39 and 41 μm, respectively, and both are very well sorted (σ_Φ <1, Walker, 1971) (see laser particle size data in the supplementary file). FPR facies occurs above and below the ash layers, without any notable textural or compositional change. In the thicker ash layer, there are three distinctive sub-layers that vary in grain size and color; the lower and upper sub-layers are light grey and finer-grained and the middle sub-layer is darker and coarser-grained.

4.4.2 Distal tephra facies

Pumice-rich tephra facies (PRT) is a crystal rich (>10% abundance; quartz + plagioclase + opaque minerals) tephra that contains weathered sub-angular to angular fragments of medium lapilli-sized pumice (~25 mm in diameter) and varied lithics. There are two types of pumice: white dense pumices that are relatively larger, and angular to sub-angular; and brown dense pumice that are more flattened. The maximum measured size and abundance of pumice clasts are 60 mm and 15-20%, respectively. Trace lithics (1%) are mostly greywacke, and are fine lapilli in size with an average diameter of 8 mm. The PRT facies occurs at Hauturu (Fig. 7b).

Pumice-poor tephra facies (PPT) comprises yellow-cream clay with traces of altered pumice and lithic clasts. The pumice fragments (8 mm) are white and make up 1–2% of the deposit. Lithic clasts comprise 2% of the deposit and their average size is approximately 10 mm in diameter. PPT was identified at Oparau Creek and Bryant Home (Fig. 7b).

Fine-grained tephra (FGT) comprises clay, characterized by white, orange, and pink alteration laminae. There is no visible pumice. The facies is crystal-rich (7%), mostly quartz, plagioclase and opaque minerals, and has been recognized at the Oparau Creek section (Fig. 7b).

4.4.3 Proximal and medial ignimbrite stratigraphy

The facies identified in the previous section are the basis for the stratigraphic variations described at the proximal-medial sites below (Fig. 3). Stratigraphic logs at each locality are presented in Fig. 9.

At Hinuera Quarry, approximately 45 km north of MVC, the Ongatiti Ignimbrite is 31 m thick and is characterised by vertical and horizontal joints (Figs. 10a and 11a). There are four facies evident (Fig. 7a): PPLP facies in the lower 14 m and characterized as a partially welded, greenish grey to grey ignimbrite and traces of carbonized wood; grading into the FPR facies in the middle 6 m, with intercalated layers of FAL facies; then an upper partially welded zone of PRLR facies

Near Tauranga, approximately 75 km northeast of MVC – the same outcrop described by Briggs et al. (1996) and dated by Briggs et al. (2005) – the Ongatiti Ignimbrite is 11 m thick (Figs. 10b and 11b). Three distinct facies were identified: PPLP (7 m thick), FPR (1 m thick), and PRLR (3 m thick), which are comparable to the facies at the Hinuera Quarry (Fig. 11a).

The Peacockes locality occurs along the Waikato riverbank, around 65 km northwest of the MVC, and comprises a nine-meter-thick deposit of non-welded, cream to yellow PRLP facies (Figs. 10c and 11c).

At Castle Rock, 25 km from the MVC, the Ongatiti Ignimbrite forms 36-m-high cliffs (Figs. 10d and 11d) of hard, dark grey, crystal-rich, and both partially welded, and vapor-phase altered ignimbrite with horizontal and vertical joints. Two facies are present, lower PRLR (25 m thick) and upper PPLP (11 m thick). The vapor-phase alteration and subsequent pumice erosion creates a 'pock-marked' outcrop appearance; however, this effect decreases with smaller pumice size and abundance from about 25 m above the base.

The exposure of the Ongatiti Ignimbrite in the Ongatiti Valley, which is approximately 30 km west of MVC, is around 25 m thick (Figs. 10e and 11e) and is massive, hard, jointed and crystal-rich comprising a lower 7 m-thick zone of PRLP facies, a middle 1 m-thick zone of FPR facies, then returning to an upper 17 m-thick zone of PRLP facies.

At Benneydale, 25 km west of MVC, a 3 m-thick deposit of Ongatiti Ignimbrite caps a hill at an elevation of approximately 600 m a.s.l. The deposit consists of hard, massive, cream-coloured, crystal-rich, partially welded ignimbrite comprising PRLP facies (Fig. 10f).

Two localities were studied on the western and eastern sides of the Waipari Gorge and collectively they are around 15 km north of the MVC, which are the most proximal sites to the source caldera. The Ongatiti Ignimbrite at Waipari Gorge west is approximately 25 m thick (Figs. 10g and 11f) and has been subdivided into lower grey, partially welded PRLR facies (at least 8 m thick), relatively more welded FPR facies (3 m thick), PRLP facies (7 m thick), and upper PPLP facies (2 m thick), showing a sharp decrease in pumice and lithic percentage and maximum size, and change in colour to brown.

At the Waipari Gorge east locality, the Ongatiti Ignimbrite is around 16 m thick, and overlies the Ngaroma Ignimbrite (Figs. 10h and 12). Part of this boundary is sharp. However, laterally the two ignimbrites are separated by a 20-cm-thick dark paleosol that grades further laterally to fluvial sediments up to 70 cm thick comprised of bedded silt and rounded, imbricated gravels (Figs. 8g and h). The Ongatiti Ignimbrite here is partially welded to welded, and cream to buff in

colour, comprising PPLR, PRLP, and FPR facies.

4.4.4 Distal tephra deposits

The internal facies characteristics of three distal deposits of the Oparau Tephra northwest of the MVC – two around Kawhia Harbour (Hauturu and Oparau Creek), both approximately 70 km WNW of the MVC, and one near Raglan (Bryant Home), approximately 90 km northwest of MVC – were documented.

At Hauturu the Oparau Tephra is approximately 7.5 m-thick (Fig. 13a) and comprises a massive, dark cream to green deposit with red and black alteration mottles and included crystals (Fig. 13b). The deposit consists of PRT facies with two white pumice rich layers, at 1 m and 2 m from the base, respectively (Fig. 14).

Near Oparau Creek, the Oparau Tephra is approximately 3 m thick, with a sharp basal contact above an underlying brown clay paleosol (Fig. 13c). The lower 25 cm comprises FGT facies, which becomes harder and changes to a yellow-cream colour into PPT facies towards the top the deposit.

At the Bryant Home section (Briggs *et al.*, 1994), the Oparau Tephra is a 50 cm thick and is a pinkish, strongly altered blocky tephra bound between an upper reddish-brown clay and a lower brown clay (Fig. 13d). PPT facies with rare white fine traces of pumice comprise this deposit.

5. Discussion

5.1 The volume of the Ongatiti eruption

We have revised the minimum deposit volume for the Ongatiti Ignimbrite to approximately 1400 km^3 as erupted, and 1000 km^3 as DRE. These volumes are a minimum because the original surface distribution of the ignimbrite has been reduced by erosion and burial by younger deposits, in particular we have not included possible, now-buried eastern and intracaldera deposits of the ignimbrite in the calculation of its areal distribution. Hence, the true area is at least double in size. The Ongatiti Ignimbrite is nearer to a low aspect ratio ignimbrite and thus based on our calculation and existing studies on other ignimbrites (such as Wilson, 1991; Cook et al., 2016) we assume that it was radially distributed around the caldera.

To qualify as a super-eruption, three criteria are commonly considered (Sparks 2005; Self 2006; Miller and Wark, 2008): (a) a mass erupted > 10^{15} kg, (b) volume of magma greater than 450 km^3, or (c) pyroclastic deposits with volumes of 1000 km^3 or more. Based on the obtained volume for the Ongatiti Ignimbrite in this study, the Ongatiti eruption can be classified as a super-eruption.

Additionally, due to comparing the estimated area and volume of the Ongatiti Ignimbrite with the new ignimbrites classification presented by Giordano and Cas (2021), the Ongatiti ignimbrite can be considered as a 'large caldera-forming ignimbrite'.

Table 2 summarizes and compares the characteristics of different ignimbrites deposited in New Zealand (Oruanui, Whakamaru, Kidnappers and Ongatiti ignimbrites) and globally. Due to the comparison two ignimbrite-forming super-eruptions are attributed to the MVC: the Ongatiti eruption and the more-voluminous 1.0 Ma Kidnappers eruption (Houghton *et al*., 1995; Wilson *et al*., 1995; Wilson *et al*., 2009) with a DRE volume of ~1200 km^3 (Cooper *et al*., 2012) (Table 2). In contrast to the Ongatiti Ignimbrite, the Kidnappers Ignimbrite is non-welded and has an underlying fall sequence (Wilson et al., 1995; Cooper et al., 2012; Cooper, 2014). The younger Whakamaru and Oruanui super-eruptions were from different caldera sources in the TVZ, but they are similar in volume (Table 2). The ignimbrite(s) of the Whakamaru eruption(s) are typically welded (Wilson, 1986; Brown *et al.*, 1998) and are probably most comparable to the Ongatiti Ignimbrite. The Oruanui ignimbrite (Wilson, 2001) on the other hand, is more comparable to the Kidnappers eruption – both are non-welded and have underlying fall deposits.

The Cerro Galan Ignimbrite (Argentina) has a similar volume and runout distance to the Ongatiti Ignimbrite and was erupted from a caldera similar in size to the Mangakino caldera (Cas et al., 2011) (Table 2); furthermore, it is also a rhyodacitic crystal-rich ignimbrite. The Peach Springs Tuff is larger in volume and consequently had a greater runout distance. On the other hand, smaller volume ignimbrites (e.g Otowi Member, New Mexico; Xáltipan Ignimbrite, Mexico) have similar runout distances. Significantly larger ignimbrites (e.g., Toba Tuff, McMullen Creek Ignimbrite, Grey's Landing Ignimbrite) are characterized by greater degrees of welding. Therefore, studying and comparing these large-volume ignimbrites in detail can provide a better understanding about flow mobility, volume and runout distance; and inferences can be made

about how these parameters affect facies characteristics.

5.2 Resolving the age of the Ongatiti eruption.

Briggs *et al.* (1996, 2005) identified the Ongatiti Ignimbrite in the Tauranga area (around Tebbutt Road) with an eruption age of 1.3 Ma. Although Cooper and Wilson (2014) acknowledged the Briggs *et al.* (2005) age, they did not extend the distribution for the Ongatiti Ignimbrite to Tauranga. Furthermore, they adopted the eruption age of Houghton *et al.* (1995) (1.21 Ma) and argued that eruption occurred after a significant time gap from zircon crystallization at 1.32 Ma. However, in light of the older eruption age of Briggs *et al.* (2005), Cooper and Wilson (2014) did acknowledge the alternative possibility that Houghton *et al.* (1995) age may need revision.

Due to the conflicting ages for the Ongatiti Ignimbrite age, we used for the first time a different dating method (i.e., zircon (U-Th)/He) on the Ongatiti Ignimbrite at Tauranga, Hinuera and Ongatiti Valley to compare with previous ages proposed by other authors (Table 1). The (U-Th)/He age near the type locality in the Ongatiti Valley (1.38 $\pm$ 0.05 Ma) matches with the (U-Th)/He age for the deposit at Tauranga (1.38 $\pm$ 0.06 Ma). The average (U-Th)/He age at Hinuera is slightly younger (1.31$\pm$ 0.09 Ma) but it is still within uncertainty of the ages at the other two localities. All of the (U-Th)/He ages are concordant with the $^{40}Ar/^{39}Ar$ age reported for the Tauranga deposit by Briggs *et al.* (2005) and support the idea that this deposit is the same eruptive unit as that of the Ongatiti Ignimbrite identified elsewhere here. Therefore, the mapped distribution to the northeast of the MVC as far as Tauranga is justified.

Our preferred age for the Ongatiti Ignimbrite due to the all-data combination, is a weighted mean age of 1.37 ±0.04 Ma (2δ) taking into account that previously published U-Pb zircon crystallization ages should be equal to or older than eruption ages. Additionally, Our new ages support continuity in age between the Ongatiti Ignimbrite in Tauranga and across other regions of the western North Island. Furthermore, all local sections of the Ongatiti Ignimbrite are vertically continuous. Hence, there is no evidence to suggest that any more than one eruption was responsible for the entire volume of the Ongatiti Ignimbrite.

5.3 Plume dynamics and flow mobility

Sparks and Wilson (1976) considered gravitational collapse of eruption columns as the source of some pyroclastic flows and that the eruption column height is the main factor that can control the original energy of the flow (Walker, 1980). Higher eruption columns that collapse generate a larger flow mobility and, therefore, a more widely distributed ignimbrite with a low aspect ratio can be created (Francis and Baker, 1977; Baker, 1981; Lube et al., 2019). The height of eruption column that controls flow mobility is ultimately controlled by the mass eruption rate hence this parameter plays a major role in determining the final runout, as well as air entrainment and depositional rate (Fisher et al., 1993; Wilson, 2001; Shimizu et al., 2019; Roche et al. 2021; Biró et al., 2022).

Based on our measurements, the Ongatiti ignimbrite has an estimated aspect ratio in the order of 1:950 to 1:1880, at the boundary between low and high aspect ratio ignimbrite (Wilson, 1991). The extensive nature of the ignimbrite as indicated by the distal tephra – which in most on-land cases are still pyroclastic flow deposits – attests to the high mobility of the Ongatiti pyroclastic flow. Thus, it is presumed here that the ignimbrite was created by one or several high eruption column(s).

One characteristic of the Ongatiti Ignimbrite is the lack of evidence for an underlying pyroclastic fall deposit, or fall succession, associated with the eruption. Potentially, a fall deposit could have been blown to the eastern side of the caldera; however, evidence for such a deposit has not been found in the Hawke's Bay region, although further work to confirm the correlation and process-origin of the Mangatewai Ti Tephra (Shane *et al*., 1996) is still required. Other reasons for the lack of a fall deposit could be either the limited exposure of the base of the ignimbrite, or that early collapse of the eruption plume restricted the accumulation of a fall deposit.

5.4 Topographic controls on ignimbrite distribution

Ignimbrites generated during plinian eruptions illustrate diverse distribution geometries ranging from ribbon-like valley-controlled deposits to semi-circular sheets emplaced by radially dispersed flows (Brown and Andrews, 2015). Antecedent topography is an important control on pyroclastic flow distribution, concentrating flows through valleys and other topographic basins. The Campo de la Piedra Pomez Ignimbrite (Cerro Blanco caldera, Argentina) is an example of a

low aspect ratio ignimbrite that split into separate flow paths through both wide valleys, narrow valleys, and narrow channels, and developed unique facies along each of these flow paths (Báez et al., 2020). Although the volume (~3.5 km^3) and runout distance (25 km) of this ignimbrite are relatively small, the concept is applied here to the scale of the Ongatiti Ignimbrite. Pyroclastic flows can also surpass topographic highs such as mountains and travel long distances including travelling over water (Brown and Andrews, 2015). Ignimbrites are mostly thick, sometimes several 100 m, within topographic basins, valleys, and calderas but thin, only a few centimeters, over hills and ridges (Brown and Andrews, 2015).

The Ongatiti ignimbrite is not exposed on the eastern side of the MVC, except at the Tauranga site located in the northeast (Fig. 3), and so the assessment of pyroclastic flow paths here focusses on the western and northern directions away from the MVC (Fig. 14). Maps of the ignimbrite deposits and profiles (Figs. 5 and 8a) show that valleys have been covered (infilled) by the Ongatiti Ignimbrite in the proximal areas (e.g., Ongatiti Valley) and also on high ridges near the caldera (west of MVC) on hills (south west of MVC) up to 900 m a.s.l (about 800 m above the caldera height) that reached by concentrated part of the pyroclastic flow. For example, the Benneydale section occurs on hills ~600 m asl, whereas at Castle Rock and Waipari Gorge (east and west) the pyroclastic flows have flowed through valleys. In contrast, the ignimbrite in medial and distal areas did not reach the highlands, filling only pre-existing lowlands, such as at Hinuera and Tauranga. In the west and northwest of the caldera, pyroclastic flows covered wide valleys between hills, and split into multiple flow lobes around paleotopographic obstacles, as well as flowing into smaller valleys.

The Waipari Gorge exposures are an example of an Ongatiti flow lobe that, after passing proximal ridges, travelled through a narrow valley, approximately 25 km from its source at the MVC. The Waipari Gorge east site is a rare example showing the basal contact with the underlying Ngaroma Ignimbrite. This contact, in part, is separated by alluvial sediments from a stream above the scoured Ngaroma Ignimbrite and a paleosol confirming a significant time gap between the Ngaroma and Ongatiti eruptions.

At the Hinuera and Tauranga sites, the pyroclastic flow passed across lowland plains, reaching the southern boundary of the Kaimai Range (Fig. 15) as shown in studies around Morrinsville

(Bowling, 1989), and also Matamata (Houghton and Cuthbertson, 1989). The southern Kaimai range – which has been uplifted along the Hauraki Fault – was present as a barrier to flow into the Bay of Plenty region. Briggs *et al.* (2005) inferred that the age of some segments of the Hauraki Fault (particularly southern segments) were older than the Ongatiti Ignimbrite (c. 1.3 Ma) but younger than the Waitеariki Ignimbrite (c. 2.09 Ma). However, the outcrop of the Ongatiti Ignimbrite near Tauranga indicates that the Ongatiti pyroclastic flow accessed the northern side of the Kaimai Range, possibly further south through low-lying paleotopography, now buried by younger ignimbrites underlying the Mamaku Plateau. Having almost a low aspect ratio, the Ongatiti Ignimbrite represents a highly mobile pyroclastic flow system.

The extinct stratovolcanoes of Pureora (1.60 ± 0.10 Ma) and Titiraupenga (1.89 ± 0.02 Ma) on the southern MVC margin (Stipp, 1968; Graham et al., 1995) and Maungatautari (1.8±0.10 Ma) NNW of the MVC margin (Robertson, 1983; Briggs, 1986; Prentice et al., 2020;), were present at the time of the Ongatiti eruption (Pittari et al., 2021). These relatively large edifices would have influenced pyroclastic flow pathways, although the extent to which these obstacles were surpassed by the pyroclastic flow is unknown. Any topographic highs that may have existed east of MVC at the time of the Ongatiti eruption have subsided due to rifting and subsequent burial in the young TVZ.

Some flow lobes reached the distal areas close to the coastline such as around Kawhia Harbour (e.g., Hauturu and Oparau Creek sites) and Raglan (Bryant Home site) where they were emplaced as the distal facies. To reach the west coast the pyroclastic flows would have encountered the Pirongia stratovolcano – a significant topographic barrier – as well having to traverse the rugged range of the western uplands.

5.5 Pyroclastic flow variations

The relationship between the Ongatiti Ignimbrite and its paleotopography suggests that there were at least three different types of pathways through which the pyroclastic flow passed from the source to distal areas. To the north and northeast (Hinuera and Tauranga sections), the pyroclastic flow passed through a wide valley and lowlands to approximately 90 km distance from the source. A vertical change from pumice-poor facies at the base to pumice-rich facies near the top indicates an energy decrease during the eruption (Wilson, 1986).

To the northwest (Waipari Gorge and Castle Rock sections), the pyroclastic flow, after leaving the caldera margin, moved through narrow valleys. The deposit began with a lower pumice-rich (PR) facies and developed into an upper pumice-poor (PP) facies. The lithic-rich (PPLR) facies near the base suggests that fluidization generated a density segregation whereby the lithics were deposited at the base and pumice clasts increased upward (Roche et al., 2001). The pumice-rich facies was observed around the Ongatiti Valley and Benneydale, to the west of MVC, although Brink (2012) also observed pumice-poor facies below pumice-rich facies in nearby areas. The ignimbrite travelled to the distal areas at least towards the west and northwest. The Peacockes section is located halfway along this pyroclastic flow path and shows pumice-rich facies.

Facies that occur in the western proximal areas and the northeastern medial areas are similar. This suggest that towards the north and northeast, the lack of hills and high lands have allowed the flow to retain its flow energy to the medial areas (to about 90 km distance from source) where its energy gradually depleted. However, in the western proximal areas (to about 30 km distance from source), after passing significant topographic barriers and ridges, the energy of the pyroclastic flow decreased earlier. Toward the northwest through the narrow valleys in proximal areas the facies sequences are distinctively pumice-poor facies overlying pumice-rich facies.

Most of the preserved sections of the ignimbrite represent areas where the Ongatiti Ignimbrite was deposited as valley-ponded facies. Figure 16 shows the parts of the pyroclastic flow system represented by each of the locality sections.

The two ash-layers identified within the FPR facies at the Hinuera Quarry represent a localized emplacement process at this site. The FPR facies above and below the ash layers are identical in texture and composition. We infer that this ash facies is related to an ash cloud surge around the pyroclastic flow, which was emplaced during local flow fluctuations. Ash cloud surges are likely to have travelled over the basal concentrated flow and approached higher topographic areas, but their deposits have been eroded or likely covered by younger deposits and were thus not observed by the authors.

5. Conclusions

The Ongatiti Ignimbrite was emplaced by a super-eruption and buried, at least much of the

western North Island as far away as Auckland and Wellington. New (U-Th)/He zircon eruption ages obtained on three samples range from c. 1.31 to 1.38 Ma, and in light of previously published U-Pb zircon crystallization ages and $^{40}Ar/^{39}Ar$ cooling ages, we adopt an age for the eruption of c. 1.37±0.04 Ma. The minimum deposit volume has been revised to approximately 1400 km^3 (~1000 km^3 DRE).

Up to around 40 km from the MVC, the ignimbrite covered both hills (up to ~ 900 m) and valleys, but beyond those distances the pyroclastic flow mainly travelled through the valleys of various widths and geometries, to more than 90 km from the vent. Ignimbrite dispersal, facies variations and internal stratigraphy were influenced by the large-scale palaeotopography. We emphasize the significance of regional palaeotopographic relief – highlands and lowlands, hill ranges and valleys – in directing the flow paths of large-volume pyroclastic flows, particularly at medial to distal parts of the runout. Correlating and recognizing the transition from proximal-medial, welded or lithified ignimbrite to distal ignimbrite (tephra) is important for understanding the overall dispersal characteristics. The modern moderate topographic relief radiating outward from the calderas of the central North Island to the North Island coastline should be an important consideration in assessing the pyroclastic flow dispersal hazard of super-eruptions.

Acknowledgement

E. Yousef Zadeh was supported by a University of Waikato Doctoral Scholarship, and internal research funds from the University of Waikato. (U-Th)/He ages were funded from a University of Waikato Strategic Investment Fund – Research (Medium) Grant. MD was supported by the AuScope NCRIS2 program and Australian Research Council (ARC) Discovery funding scheme (DP160102427). We would like to express our gratitude to colleagues from the University of Waikato who helped us to complete this research. The paper is also an output of the Commission on Tephrochronology (COT) of the International Association of Volcanism and Chemistry of the Earth's Interior (IAVCEI). Thank you to Geoff Lerner and an anonymous reviewer for their helpful comments on the manuscript.

References

Allan, A.S., Baker, J.A., Carter, L. and Wysoczanksi, R.J., 2008. Reconstructing the Quaternary evolution of the world's most active silicic volcanic system: insights from an~ 1.65 Ma deep ocean tephra record sourced from Taupo Volcanic Zone, New Zealand. Quaternary Science Reviews, 27(25): 2341-2360.

Alloway, B., Westgate, J., Pillans, B., Pearce, N., Newnham, R., Byrami, M. and Aarburg, S., 2004. Stratigraphy, age and correlation of middle Pleistocene silicic tephras in the Auckland region, New Zealand: a prolific distal record of Taupo Volcanic Zone volcanism. New Zealand Journal of Geology and Geophysics, 47(3): 447-479.

Alloway, B.V., Pillans, B.J., Carter, L., Naish, T.R. and Westgate, J.A., 2005. Onshore–offshore correlation of Pleistocene rhyolitic eruptions from New Zealand: implications for TVZ eruptive history and paleoenvironmental construction. Quaternary Science Reviews, 24(14-15): 1601-1622.

Aydin, A. and DeGraff, J.M., 1988. Evolution of polygonal fracture patterns in lava flows. Science, 239(4839): 471-476.

Báez, W., Bustos, E., Chiodi, A., Reckziegel, F., Arnosio, M., de Silva, S., Giordano, G., Viramonte, J., Sampietro-Vattuone, M. and Peña-Monné, J., 2020. Eruptive style and flow dynamics of the pyroclastic density currents related to the Holocene Cerro Blanco eruption (Southern Puna plateau, Argentina). Journal of South American Earth Sciences, 98: 102482.

Baker, M.J., 1981. The nature and distribution of upper Cenozoic ignimbrite centres in the Central Andes. Journal of Volcanology and Geothermal Research, 11(2-4): 293-315.

Barton, N., 1978. Suggested methods for the quantitative description of discontinuities in rock masses. ISRM, International Journal of Rock Mechanics and Mining Sciences & Geomechanics Abstracts, 15(6): 319-368.

Biró, T., Hencz, M., Telbisz, T., Ceri, Z. and Karátson, D., 2022. The relationship between ignimbrite lithofacies and topography in a foothill setting formed on Miocene pyroclastics–a case study from the Bükkalja, Northern Hungary. Hungarian Geographical Bulletin, 71(3), pp.213-229.

Black, T.M., Shane, P.A., Westgate, J.A. and Froggatt, P.C., 1996. Chronological and palaeomagnetic constraints on widespread welded ignimbrites of the Taupo volcanic zone, New Zealand. Bulletin of volcanology, 58(2): 226-238.

Bowling, F.M., 1989. Volcanic geology of ignimbrites on the western margin of the Hauraki Depression and in the Mangatangi area. Unpublished MSc thesis, University of Waikato, Hamilton.

Briggs, N.D., 1976. Recognition and correlation of subdivisions within the Whakamaru Ignimbrite, central North Island, New Zealand. New Zealand Journal of Geology and Geophysics, 19(4): 463-501.

Briggs, R., Gifford, M., Moyle, A., Taylor, S., Norman, M., Houghton, B. and Wilson, C., 1993. Geochemical zoning and eruptive mixing in ignimbrites from Mangakino volcano, Taupo Volcanic Zone, New Zealand. Journal of volcanology and geothermal research, 56(3): 175-203.

Briggs, R.M., Lowe, D.J., Goles, G.G. and Shepherd, T.G., 1994. Intra-conference Tour Day 1: Hamilton–Raglan–Hamilton. In: Lowe, D.J. (ed), 'Conference Tour Guides'. Proceedings

International Inter-INQUA Field Conference on Tephrochronology, Loess, and Paleopedology, University of Waikato, Hamilton, New Zealand, pp. 24-44.

Briggs, R.M., 1986. Petrology and geochemistry of Maungatautari, a medium-K andesite-dacite volcano. New Zealand journal of geology and geophysics, 29(3): 273-289.

Brink, M.T., 2012. Emplacement processes of ignimbrites in the Ongatiti Valley, southeast Te Kuiti. Unpubslished MSc thesis, University of Waikato, Hamilton.

Brown, R.J. and Andrews, G.D., 2015. Deposits of pyroclastic density currents, The encyclopedia of volcanoes. Elsevier, pp. 631-648.

Brown, S., Wilson, C., Cole, J., Wooden, J.J.J.o.V. and Research, G., 1998. The Whakamaru group ignimbrites, Taupo Volcanic Zone, New Zealand: evidence for reverse tapping of a zoned silicic magmatic system. Journal of volcanology and geothermal research, 84(1-2): 1-37.

Brown, S.J. and Smith, R.T., 2004. Crystallisation history and crustal inheritance in a large silicic magma system: 206Pb/238U ion probe dating of zircons from the 1.2 Ma Ongatiti ignimbrite, Taupo Volcanic Zone. Journal of Volcanology and Geothermal Research, 135(3): 247-257.

Cas, R. and Wright, J., 1987. Volcanic successions: Ancient and modern. Allen and Unin, London.

Cas, R.A., Wright, H.M., Folkes, C.B., Lesti, C., Porreca, M., Giordano, G. and Viramonte, J.G., 2011. The flow dynamics of an extremely large volume pyroclastic flow, the 2.08-Ma Cerro Galán Ignimbrite, NW Argentina, and comparison with other flow types. Bulletin of Volcanology, 73(10): 1583-1609.

Cavazos-Álvarez, J.A. and Carrasco-Núñez, G., 2019. Effective mapping of large ignimbrites by using a GIS-based methodology; case of the Xáltipan ignimbrite from Los Humeros caldera, Mexico. Terra Digitalis, 3(2), pp.1-8.

Chesner, C., Rose, W., 1991. Stratigraphy of the Toba Tuffs and the evolution of the Toba Caldera Complex, Sumatra, Indonesia. Bulletin of Volcanology, 53: 343–356

Cook, G.W., Wolff, J.A. and Self, S., 2016. Estimating the eruptive volume of a large pyroclastic body: the Otowi Member of the Bandelier Tuff, Valles caldera, New Mexico. Bulletin of Volcanology, 78(2): 10.

Cooper, G.F., 2014. The dynamics of large-scale silicic magmatic systems: case studies from Mangakino Volcanic Centre, Taupo Volcanic Zone, New Zealand, Victoria University of Wellington.

Cooper, G.F. and Wilson, C.J., 2014. Development, mobilisation and eruption of a large crystal-rich rhyolite: the Ongatiti ignimbrite, New Zealand. Lithos, 198: 38-57.

Cooper, G.F., Wilson, C.J., Charlier, B.L., Wooden, J.L. and Ireland, T.R., 2014. Temporal evolution and compositional signatures of two supervolcanic systems recorded in zircons from Mangakino volcanic centre, New Zealand. Contributions to Mineralogy and Petrology, 167(6): 1018.

Cooper, G.F., Wilson, C.J., Millet, M.-A., Baker, J.A. and Smith, E.G., 2012. Systematic tapping of independent magma chambers during the 1 Ma Kidnappers supereruption. Earth and Planetary Science Letters, 313: 23-33.

Danišík, M., Lowe, D.J., Schmitt, A.K., Friedrichs, B., Hogg, A.G. and Evans, N.J., 2020. Sub-millennial eruptive recurrence in the silicic Mangaone Subgroup tephra sequence, New Zealand, from Bayesian modelling of zircon double-dating and radiocarbon ages. Quaternary Science Reviews, 246, p.106517.

DeGraff, J.M. and Aydin, A., 1987. Surface morphology of columnar joints and its significance to mechanics and direction of joint growth. Geological Society of America Bulletin, 99(5): 605-617.

Edbrooke, S., 2005. Geology of the Waikato area, geological map, scale 1: 250,000. GNS Science, Lower Hutt, New Zealand.

Farley, K.A., Wolf, R.A., Silver, L.T., 1996. The effects of long alpha-stopping distances on (U-Th)/He ages. Geochimica et Cosmochimica Acta. 60(21): 4223-4229.

Fattahi, M. and Stokes, S., 2000. Extending the time range of luminescence dating using red TL (RTL) from volcanic quartz. Radiation Measurements, 32: 479-485.

Fisher, R.V. and Schmincke, H.U., 1984. Pyroclastic rocks. Springer-Verlag.

Francis, P. and Baker, M.J.N., 1977. Mobility of pyroclastic flows. Nature, 270(5633): 164.

Freundt, A., Wilson, C. and Carey, S., 2000. Ignimbrites and block-and-ash flow deposits. In: Encyclopedia of volcanoes. , ed. by Sigurdsson, H.. Academic Press, New York, pp. 581-599.

Giordano, G. and Cas, R.A., 2021. Classification of ignimbrites and their eruptions. Earth-Science Reviews: 103697.

Graham, I., Cole, J., Briggs, R., Gamble, J. and Smith, I., 1995. Petrology and petrogenesis of volcanic rocks from the Taupo Volcanic Zone: a review. Journal of volcanology and geothermal research, 68(1-3): 59-87.

Healy, J., 1964. Volcanic mechanisms in the Taupo Volcanic Zone, New Zealand. New Zealand journal of geology and geophysics, 7(1): 6-23.

Heron, D.W., 2014. Geological Map of New Zealand 1:250 000. GNS Science Geological Map 1. Lower Hutt, New Zealand. GNS Science.

Hopkins, J.L., Lowe, D.J., Horrocks, J.H. 2021. Tephrochronology in Aotearoa New Zealand. *New* Zealand Journal of Geology and Geophysics, 64 (2/3): 153-200.

Horrocks, J.L., 2000. Stratigraphy, chronology and correlation of the Plio-Pleistocene (c. 2.2-0.8 Ma) Kauroa ash sequence, western central North Island, New Zealand, Unpublished Ph.D. thesis, University of Waikato, Hamilton.

Houghton, B. and Cuthbertson, A., 1989. Sheet T14BD Kaimai; Geological Map of New Zealand 1: 50,000. Dept. Sci. Indus. Res., Wellington, New Zealand.

Houghton, B., Wilson, C., McWilliams, M., Lanphere, M., Weaver, S., Briggs, R. and Pringle, M., 1995. Chronology and dynamics of a large silicic magmatic system: central Taupo Volcanic Zone, New Zealand. Geology, 23(1): 13-16.

Kear, D., 1960. Sheet 4 Hamilton "Geological Map of New Zealand", 1: 250,000. Department of Scientific and Industrial Research, Wellington, New Zealand.

Knott, T.R., Branney, M.J., Reichow, M.K., Finn, D.R., Coe,R.S., Storey, M., Barfod, D., McCurry, M., 2016. Mid-Miocene record of large-scale Snake River–type explosive volcanism and associated subsidence on the Yellowstone hotspot track: The Cassia Formation of Idaho, USA. *GSA Bulletin* 2016;; 128 (7-8): 1121–1146. doi

Knott,T.R., Branney, M.J., Reichow, M.K., Finn, D.R., Tapster, S., Coe. R., 2020. Discovery of two new super-eruptions from the Yellowstone hotspot track (USA): Is the Yellowstone hotspot waning?. Geology*;* 48 (9): 934–938

Leonard, G., Begg, J., Wilson, C. and Leonard, G., 2010. Institute of Geological and Nuclear Sciences 1: 250,000 geological map 5. 1 sheet and 99 pp. Institute of Geological and Nuclear Sciences, Lower Hutt.

Lipman, P.W., 1984. The roots of ash flow calderas in western North America: windows into the

tops of granitic batholiths. Journal of Geophysical Research: Solid Earth, 89(B10): 8801-8841.

Lowe, D.J., Tippett, J.M., Kamp, P.J., Liddell, I.J., Briggs, R.M. and Horrocks, J.L., 2001. Ages on weathered Plio-Pleistocene tephra sequences, western North Island, New Zealand. Les Dossiers de l'Archeo-Logis, 1: 45-60.

Lube, G., Breard, E.C., Jones, J., Fullard, L., Dufek, J., Cronin, S.J. and Wang, T., 2019. Generation of air lubrication within pyroclastic density currents. Nature Geoscience, 12(5): 381-386.

Martin, R.C., 1961. Stratigraphy and structural outline of the Taupo Volcanic Zone. New Zealand journal of geology and geophysics, 4(4): 449-478.

Mason, B.G., Pyle, D.M. and Oppenheimer, C., 2004. The size and frequency of the largest explosive eruptions on Earth. Bulletin of Volcanology, 66(3): 735-748.

McCormack, K.D., Gee, M.M., McNaughton, N.J., Smith, R. and Fletcher, I.R., 2009. U–Pb dating of magmatic and xenocryst zircons from Mangakino ignimbrites and their correlation with detrital zircons from the Torlesse metasediments, Taupo Volcanic Zone, New Zealand. Journal of Volcanology and Geothermal Research, 183(1): 97-111.

Mildenhall, D. and Alloway, B., 2008. A widespread ca. 1.1 Ma TVZ silicic tephra preserved near Wellington, New Zealand: implications for regional reconstruction of mid-Pleistocene vegetation. Quaternary International, 178(1): 167-182.

Miller, C.F. and Wark, D.A., 2008. Supervolcanoes and their explosive supereruptions. Elements, 4(1): 11-15.

Moon, V.G., 1989. Relationships between the geomechanics and petrography of ignimbrite, Unpublished Ph.D. thesis, University of Waikato, Hamilton.

Moon, V.G., 1993. Geotechnical characteristics of ignimbrite: A soft pyroclastic rock type. Engineering Geology, 35(1-2): 33-48.

Pain, C., 1975. Some tephra deposits in the south-west Waikato area, North Island, New Zealand. New Zealand journal of geology and geophysics, 18(4): 541-550.

Pittari, A., Cas, R.A.F., Edgar, C.J., Nichols, H.J., Wolff, J.A. and Martí, J., 2006. The influence of palaeotopography on facies architecture and pyroclastic flow processes of a lithic-rich ignimbrite in a high gradient setting: the Abrigo Ignimbrite, Tenerife, Canary Islands. Journal of Volcanology and Geothermal Research, 152(3-4): 273-315.

Pittari, A., Prentice, M.L., McLeod, O.E., Yousef Zadeh, E., Kamp, P.J., Danišík, M. and Vincent, K.A., 2021. Inception of the modern North Island (New Zealand) volcanic setting: spatio-temporal patterns of volcanism between 3.0 and 0.9 Ma. New Zealand Journal of Geology and Geophysics, 64 (2/3): 250-272,

Prentice, M.L., Pittari, A., Barker, S.L. and Moon, V.G., 2020. Volcanogenic processes and petrogenesis of the early Pleistocene andesitic-dacitic Maungatautari composite cone, central Waikato, New Zealand. New Zealand Journal of Geology and Geophysics, 63(2): 210-226.

Pringle, M., McWilliams, M., Houghton, B.F., Lanphere, M. and Wilson, C., 1992. 40Ar/39Ar dating of Quaternary feldspar: examples from the Taupo Volcanic Zone, New Zealand. Geology, 20(6): 531-534.

Pyle, D.M., 1995. Assessment of the minimum volume of tephra fall deposits. Journal of Volcanology and Geothermal Research, 69(3-4): 379-382.

Robertson, D.J., 1983. Paleomagnetism and geochronology of volcanics in the northern North Island, New Zealand, ResearchSpace, University of Auckland.

Roche, o., Azzaoui, N., Guillin,A., 2021. Discharge rate of explosive volcanic eruption controls runout distance of pyroclastic density currents. Earth and Planetary Science Letters, 571: 117-114

Roche, o., Buesch, D. C., Valentine, G. A., 2016. Slow-moving and far-travelled dense pyroclastic flows during the Peach Spring super-eruption, Nature Communications. 10890

Roche, O., Druitt, T. and Cas, R., 2001. Experimental aqueous fluidization of ignimbrite. Journal of Volcanology and Geothermal Research, 112(1-4): 267-280.

Rogan, M., 1982. A geophysical study of the Taupo volcanic zone New Zealand. Journal of Geophysical Research: Solid Earth, 87(B5): 4073-4088.

Rose, W. and Chesner, C., 1987. Dispersal of ash in the great Toba eruption, 75 ka. Geology, 15(10): 913-917.

Self, S., 2006. The effects and consequences of very large explosive volcanic eruptions. Philosophical Transactions of the Royal Society A: Mathematical, Physical and Engineering Sciences, 364(1845): 2073-2097.

Shane, P.A., Black, T.M., Alloway, B.V. and Westgate, J.A., 1996. Early to middle Pleistocene tephrochronology of North Island, New Zealand: Implications for volcanism, tectonism, and paleoenvironments. Geological Society of America Bulletin, 108(8): 915-925.

Shimizu, H.A., Koyaguchi, T. and Suzuki, Y.J., 2019. The run-out distance of large-scale pyroclastic density currents: a two-layer depth-averaged model. Journal of Volcanology and Geothermal Research, 381, pp.168-184.

Soengkono, S., Hochstein, M., Smith, I. and Itaya, T., 1992. Geophysical evidence for widespread reversely magnetised pyroclastics in the western Taupo Volcanic Zone (New Zealand). New Zealand Journal of Geology and Geophysics, 35(1): 47-55.

Sparks, R., Self, S., Grattan, J., Oppenheimer, C., Pyle, D. and Rymer, H., 2005. Super-eruptions: Global effects and future threats: London, UK, Report of a Geological Society of London working group. Web edition available at www.geolsoc.org.uk/supereruptions

Sparks, R. and Walker, G., 1977. The significance of vitric-enriched air-fall ashes associated with crystal-enriched ignimbrites. Journal of Volcanology and Geothermal Research, 2(4): 329-341.

Sparks, R. and Wilson, L., 1976. A model for the formation of ignimbrite by gravitational column collapse. Journal of the Geological Society, 132(4): 441-451.

Stern, T., 1979. Regional and residual gravity fields, central North Island, New Zealand. New Zealand journal of geology and geophysics, 22(4): 479-485.

Stipp, J.J., 1968. The geochronology and petrogenesis of the Cenozoic volcanics of the North Island, New Zealand. Unpublished Ph.D. thesis, The Australian National University, Canberra.

Vandergoes, M.J., Hogg, A.G., Lowe, D.J., Newnham, R.M., Denton, G.H., Southon, J., Barrell, D.J.A., Wilson, C.J.N., McGlone, M.S., Allan, A.S.R., Almond, P.C., Petchey, F., Dalbell, K., Dieffenbacher-Krall, A.C., and Blaauw, M., 2013. A revised age for the Kawakawa/Oruanui tephra, a key marker for the Last Glacial Maximum in New Zealand. Quaternary Science Reviews, 74: 195-201.

Walker, G.P., 1980. The Taupo pumice: product of the most powerful known (ultraplinian) eruption? Journal of volcanology and geothermal research, 8(1): 69-94.

Walker, G.P., 1983. Ignimbrite types and ignimbrite problems. Journal of Volcanology and Geothermal Research, 17(1-4): 65-88.

Westgate, J. A., Pearce, N. J. G., Perkins, W. T., Preece, S. J., Chesner, C. A., Muhammad, R. F., 2013. Tephrochronology of the Toba tuffs: four primary glass populations define the 75-ka Youngest Toba Tuff, northern Sumatra, Indonesia. J. Quaternary Sci., 28: 772-776.

Wilson, C., 1986. Reconnaissance stratigraphy and volcanology of ignimbrites from Mangakino volcano. Late Cenozoic volcanism in New Zealand. Royal Society of New Zealand Bulletin, 23: 179-193.

Wilson, C., 1991. Ignimbrite morphology and the effects of erosion: a New Zealand case study. Bulletin of Volcanology, 53(8): 635-644.

Wilson, C., Charlier, B., Fagan, C., Spinks, K., Gravley, D., Simmons, S. and Browne, P., 2008. U–Pb dating of zircon in hydrothermally altered rocks as a correlation tool: application to the Mangakino geothermal field, New Zealand. Journal of Volcanology and Geothermal Research, 176(2): 191-198.

Wilson, C., Charlier, B., Rowland, J. and Browne, P., 2010. U–Pb dating of zircon in subsurface, hydrothermally altered pyroclastic deposits and implications for subsidence in a magmatically active rift: Taupo Volcanic Zone, New Zealand. Journal of Volcanology and Geothermal Research, 191(1-2): 69-78.

Wilson, C., Gravley, D., Leonard, G. and Rowland, J., 2009. Volcanism in the central Taupo Volcanic Zone, New Zealand: tempo, styles and controls. Studies in Volcanology: The Legacy of George Walker. Special Publications of IAVCEI, 2: 225-247.

Wilson, C., Houghton, B., Kampt, P. and McWilliams, M., 1995a. An exceptionally widespread ignimbrite with implications for pyroclastic flow emplacement. Nature, 378(6557): 605-607.

Wilson, C., Houghton, B. and Lloyd, E., 1986. Volcanic history and evolution of the Maroa-Taupo area, central North Island, Late Cenozoic Volcanism in New Zealand. Royal Society of New Zealand Bulletin, 23:194-223.

Wilson, C., Houghton, B., McWilliams, M., Lanphere, M., Weaver, S. and Briggs, R., 1995b. Volcanic and structural evolution of Taupo Volcanic Zone, New Zealand: a review. Journal of volcanology and geothermal research, 68(1-3): 1-28.

Wilson, C., Rogan, A., Smith, I., Northey, D., Nairn, I. and Houghton, B., 1984. Caldera volcanoes of the Taupo volcanic zone, New Zealand. Journal of Geophysical Research: Solid Earth, 89(B10): 8463-8484.

Wilson, C.J., 2001. The 26.5 ka Oruanui eruption, New Zealand: an introduction and overview. Journal of Volcanology and Geothermal Research, 112(1-4): 133-174.

Wilson, C.J. and Rowland, J.V., 2016. The volcanic, magmatic and tectonic setting of the Taupo Volcanic Zone, New Zealand, reviewed from a geothermal perspective. Geothermics, 59: 168-187.

Figure Captions

Figure 1: Proximal and distal features of the Mangakino Volcanic Centre (MVC). (a) Photograph of the plateau that lies geographically above the Mangakino Caldera towards the southwestern caldera rim, showing the slightly older andesitic cones of Titiraupenga and Pureora

(left), the raised plateau underlain by outflow ignimbrites from the Mangakino and much younger Whakamaru calderas (centre background), and raised Jurassic basement ranges (left). The plain in the foreground is underlain by post-MVC Whakamaru Ignimbrite, and younger pyroclastics, which now infill and bury the Mangakino Caldera. (b) The location of distal tephra equivalents of the Ongatiti Ignimbrite: Ongatiti Tephra near Auckland (yellow dots, studied by Alloway *et al*. 2004); equivalent tephras near Wellington (Transmission Gully, TG, Mildenhall and Alloway, 2008), drill cores in the Pacific Ocean (AT311 tephra, Alloway *et al*., 2005), and near Hawke's Bay (Mangatwaiiti Tephra, MT, Shane *et al*., 1996) (white squares); and distal sites investigated in this study (pink circles). Dark red areas show the Ongatiti Ignimbrite in proximal and medial areas and the red line is the estimated western boundary of MVC. Basemap from Google Earth https://www.google.com/earth/.

Figure 2: A digital elevation model (DEM) of the areas near Mangakino Volcanic Centre (MVC) and the distribution of the outflow deposits of the Ongatiti Ignimbrite. Three profiles AA', BB', and CC' represent the above sea level in meters (vertical axes) versus the horizontal distance (in meters) across the MVC. Red line is the exposed MVC caldera rim.

Figure 3**:** Distribution of the Ongatiti Ignimbrite (blue), caldera position (red dotted line), Geological features (black) and field study sites (purple circles). The co-ordinates for the field study sites are: Benneydale (362934.11 E, 5737924.32 S), Ongatiti Valley (351577.00 E, 5748692.00 S), Waipari Gorge East (373563.00 E, 5767471.00 S), Waipari Gorge West (373588.00 E, 5768146.00 S), Castle Rock (T16, 370326.00 E, 5778629.00 S), Oparau Creek (317372.824 E, 5786115.186 S), Hauturu (318828.035 E, 5781688.093 S), Hinuera (384201.00 E, 5802482.00 S), Peacocke (S14, 352598.16 E, 5813043.55 S), Bryant Home (308244.681 E, 5811321.485S), and Tauranga (U14, 417219.00 E, 5821442.00 S).

Figure 4: Map of the Ongatiti Ignimbrite illustrating the 'expected' and 'reliable' distribution zones based on GIS data and sites studied here. The 'reliable' zone (green areas) is defined by the distributions mapped in QMAP (Edbrooke, 2005; Leonard et al., 2010).

Figure 5: Topographic profiles (AA' to FF') of elevation versus distance (metres) from the caldera margin in different directions radially around the western side of the MVC. The thick red lines on the profiles are the locations of present-day Ongatiti Ignimbrite exposure. The map

shows the locations of each profile.

Figure 6: Plots of (a) runout distance versus volume, and (b) volume versus mean mass discharge rate, showing the position of the Ongatiti Ignimbrite (green dot) within the range of concentrated pyroclastic density current deposits (orange distribution) and best-fit lines presented by Roche et al. (2021) (based on figs. 8a and b of Roche et al., 2021).

Figure 7**:** a) Stratigraphic logs of the Ongatiti Ignimbrite at proximal-medial sites illustrating the vertical and lateral distribution of the different facies. b) Stratigraphic logs of the Oparau Tephra at distal sites. HR: Hauturu; OC: Oparau Creek; BH: Bryant Home. See text for the definition of facies abbreviations.

Figure 8: Facies characteristics of proximal-medial deposits of the Ongatiti Ignimbrite. (a) Close up from PRLR facies at Tauranga. (b) PRLP facies in the Ongatiti Valley. (c) FPR facies at Waipari Gorge East. (d) PPLP facies at the Hinuera Quarry section. (e) PPLR facies at the base of the Ongatiti Ignimbrite at Waipari Gorge East. (f) Ash layer in middle of the Hinuera Quarry section. (g) Fluvial gravel and siltstone that occurs between the upper Ngaroma and lower Ongatiti ignimbrites at Waipari Gorge east. This deposit, which grades laterally to (h) a paleosol.

Figure 9: Types of pumice (a) at Hinuera - 1 is a yellow vesicular pumice, 2 is a cream woody pumice; and (b) in the Ongatiti Valley – 3 is a vesicular pumice and 4 is a flattened pumice.

Figure 10: Stratigraphic logs of the Ongatiti Ignimbrite including vertical profiles of pumice abundance (PA), pumice aspect ratio (AR), maximum pumice size (MPS), lithic abundance (LA) and maximum lithic size (MLS) at each of the proximal-medial localities: (a) Hinuera, (b) Tauranga, (c) Peacocke, (d) Castle Rock, (e) Ongatiti Valley, (f) Benneydale, (g) Waipari Gorge west, and (h) Waipari Gorge east

Figure 11: Outcrop morphology and exposure at: (a) Hinuera Quarry, (b) Tauranga section, (c) Peacockes, (d) Castle Rock, (e) Ongatiti Valley, and (f) Waipari Gorge west.

Figure 12: Photo and a sketch of the Waipari Gorge east outcrop viewed toward the north showing the contact relationships between the lower Ngaroma Ignimbrite, middle paleosol and river sediments, and the upper Ongatiti Ignimbrite and a fallen block of the Ahuroa Ignimbrite (Ahuroa Ignimbrite hidden behind the vegetation).

Figure 13: Distal Ongatiti-equivalent tephras showing: (a) the Hauturu outcrop, and (b) close up of the same showing trace pumice and lithic clast within PRT facies; (c) the boundary between the Oparau Tephra and underlying brown paleosol at Oparau Creek; and (d) Bryant Home section.

Figure 14: Stratigraphic log from the Hauturu section showing pumice abundance (PA), aspect ratio (AR), maximum pumice size (MPS), lithic abundance (LA), and maximum lithic size (MLS).

Figure 15: Map representing the position of the caldera and some main topographic barriers (ridges and high lands) to the pyroclastic flow. Arrows show flow directions: thicker arrows are the main flow directions, thin arrows as minor flow lobes, dotted arrows represent flows in distal areas.

Figure 16: Schematic cross-section through a paleo-valley beneath the Ongatiti pyroclastic flow showing different facies: Pumice- and lithic-poor (PPLP), pumice-rich, lithic-poor (PRLP), pumice- and lithic-rich (PRLR). Modified after Pittari et al. (2006a). B, Benneydale; WW, Waipari Gorge west; WE, Waipari Gorge east; OV, Ongatiti valley; C, Castle Rock; P, Peacockes; H, Hinuera; TA, Tauranga. The rectangles refer to the stratigraphic logs shown in figures 7 and 10.

Table 1: A summary of published age data for the Ongatiti Ignimbrite and its distal correlatives, and the new (U-Th)/He ages from this study.

Method		Age (Ma) ± error	Author	Age Group
K/Ar on hornblende		1.25 ± 0.09	Soengkono *et al.* (1992)	IA
$^{40}Ar/^{39}Ar$ on feldspar	(plateau age)	1.21 ± 0.04, 1σ	Houghton *et al.* (1995)[a]	
Isothermal plateau fission track on glass		1.25 ± 0.12, 1σ	Black *et al.* (1996)	
Red thermoluminescence in quartz		1.280 ± 0.165	Fattahi and Stokes (2000)	
$^{40}Ar/^{39}Ar$ on feldspar	(plateau age) (isochron age)	1.32 ± 0.01, 1σ 1.34 ± 0.02, 1σ	Briggs *et al.* (2005)	IB
U-Pb on zircon		1.31 ± 0.03, 95% CI	Brown and Smith (2004)	II
U-Pb on zircon		1.30 ± 0.12, 2σ	Wilson et al. (2008)	
U-Pb on zircon		1.29 ± 0.07, 95% CI	McCormack *et al.* (2009)	
U-Pb on zircon	mean all analyses mean of rims	1.32 ± 0.01, 2σ 1.28 ± 0.02, 2σ	Cooper *et al.* (2014)	
Zircon fission track (n = 29)		1.28 ± 0.11, 1σ	Leonard *et al.* (2001)[b]	III
Isothermal plateau fission track on glass		1.14 ± 0.06, 1σ 1.29 ± 0.14, 1σ	Alloway *et al.* (2004)[c]	
Isothermal plateau fission track on glass		1.21 ± 0.08, 1s 1.18 ± 0.09, 1s	Mildenhall and Alloway (2008)[d]	
Graphically correlated		1.202	Alloway *et al.* (2005)[e]	
$^{40}Ar/^{39}Ar$ on feldspar		1.24 ± 0.07	Shane *et al.* (1996)[f]	
Isothermal plateau fission track on glass		1.23 ± 0.09, 1s	Shane *et al.* (1996)[f]	
(U-Th)/He on zircon	Hinuera	1.314 ± 0.086, 2σ	This study	IV
	Tauranga	1.277 ± 0.061, 2σ		
	Ongatiti Valley	1.382 ± 0.052, 2σ		

[a]This age supercedes earlier $^{40}Ar/^{39}Ar$ ages for the Ongatiti Ignimbrite from the same research team of 1.251 ± 0.060 Ma by Pringle *et al.* (1992) and 1.23 ± 0.02 Ma cited by Briggs *et al.* (1993). Pringle *et al.* (1992) states the error as an estimate of the standard deviation of the analytical precision.
[b]Kauroa ash bed K12 (Raglan), equivalent to the Oparau Tephra (see Hopkins *et al.*, 2021)
[c]Ongatiti Tephra studied at Ohakuri
[d]Tephra (AT-62 and AT-63) at the Patiki core site.
[e]Tephra AT-311 in ODP (site 1124)
[f]Mangatewaiiti Tephra (Hawke's Bay), tentative correlation to Ongatiti Ignimbrite (Shane *et al.*, 1996)

Table 2: Comparison of ignimbrite-forming supereruptions of the Taupo Volcanic Zone, and a global example.

Eruption	Age	Volume (km^3 DRE)	Source caldera	Runout distance (km)	Characteristics	Reference
Supereruptions of the Taupo Volcanic Zone						
Oruanui	25.4ka	~530	Taupo	~90 km > 200 m	Produced fall deposits and PDC	(Wilson, 2001)
Whakamaru group	330-340ka	>1000	Whakamaru	>60 km	Varied due to different ignimbrites	(Wilson et al., 1986); (Brown et al., 1998)
Kidnappers	1Ma	1200	Mangakino	~190 km	Initial pyroclastic fall deposit; overlying non-welded, lithic- and crystal-rich ignimbrite	Cooper *et al.* (2012) Wilson *et al.* (1995)
Ongatiti	1.3Ma	~1000 (1400 vol)	Mangakino	~90 km	Crystal-rich, pumice- rich rhyodacitic ignimbrite.	This study Cooper and Wilson (2014) Briggs *et al.* (1993)
Comparable global supereruption						
Cerro Galan (Argentina)	2080	>630	Cerro Galan	~100 km	Rhyodacitic, crystal-rich, pumice- and lithic-poor ignimbrite	Cas *et al.* (2011)
Otowi Member (New Mexico, USA)	1.6 Ma	216-550	Valles caldera	<90 km	Member of the Bandelier Tuff; included Plinian and coignimbrite fall deposits, outflow and intracaldera ignimbrite.	Cook *et al.* (2016)
Peach Springs Tuff (USA)	18.8 Ma	1300	Silver Creek caldera	>170 km	Ignimbrite ranges from non-welded to densely welded. Vitric to crystallized; contains lithic fragments >10cm.	Roche *et al.* (2016)
Toba tuff (Indonesia)	75 ka (Youngest) 1.2 Ma (oldest)	2500-3000	Toba caldera		Comprises three welded and nonwelded tuffs.	Chesner *et al.* (1991) Westgate *et al.* (2013)
McMullen Creek Ignimbrite	8.99 Ma	>1700	Yellowstone caldera		Comprises two dark intensely welded zones and a pale, less-welded center.	Knott et al. (2016 & 2020)

Grey's Landing Ignimbrite	8.72 Ma	⩾2800	Yellowstone caldera		Rhyolitic mostly intense welded, with original vitroclast outlines	Knott et al. (2020)
Xáltipan Ignimbrite (Mexico)	~50ka	>344	Los Humeros caldera	Max ~59km	Composed of two flow units separated by a pumice fall layer and a basal pumice fall.	Cavazos-Álvarez and Carrasco-Núñez (2019)

Declaration of interests

☒The authors declare that they have no known competing financial interests or personal relationships that could have appeared to influence the work reported in this paper.

☐The authors declare the following financial interests/personal relationships which may be considered as potential competing interests:

Highlights:

- The Ongatiti Ignimbrite was emplaced by a super-eruption.
- New (U-Th)/He zircon eruption ages obtained an age of c. 1.37±0.04 Ma.
- The minimum deposit volume has been revised to approximately 1400 km^3 (~1000 km^3 DRE).
- The pyroclastic flow mainly travelled through valleys of various widths and geometries, to more than 90 km from the vent.
- Ignimbrite dispersal, facies variations and internal stratigraphy were influenced by the large-scale palaeotopography.

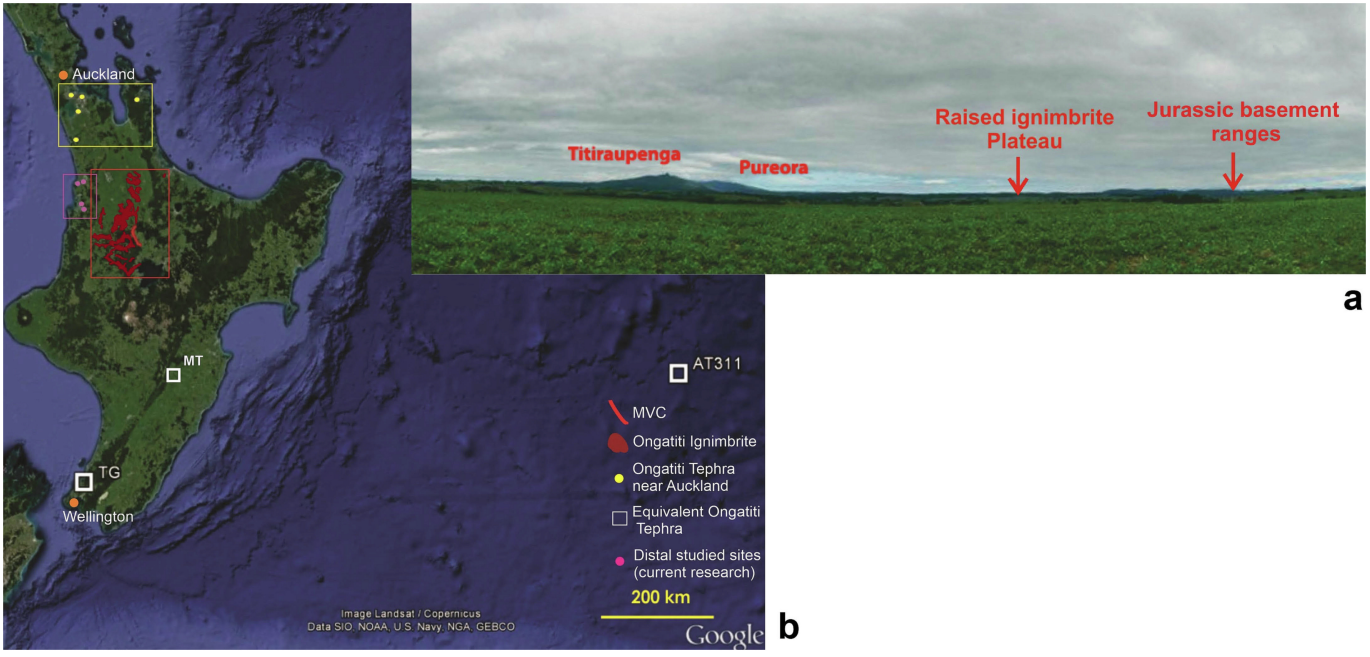
Titiraupenga
Pureora
Raised ignimbrite Plateau
Jurassic basement ranges
a
Auckland
MT
TG
Wellington
AT311
MVC
Ongatiti Ignimbrite
Ongatiti Tephra near Auckland
Equivalent Ongatiti Tephra
Distal studied sites (current research)
200 km
Image Landsat / Copernicus
Data SIO, NOAA, U.S. Navy, NGA, GEBCO
Google
b

Figure 1

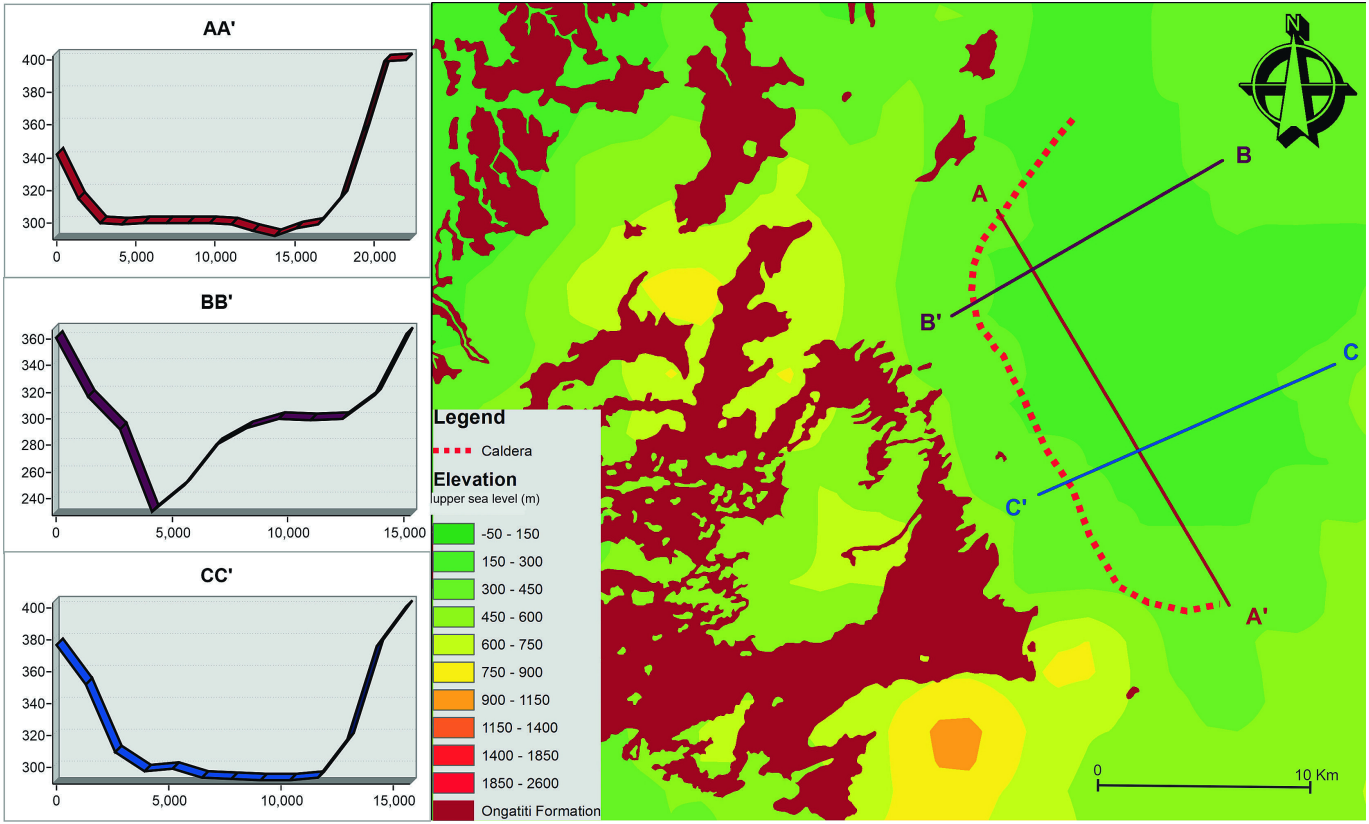
AA'
400
380
360
340
320
300
0
5,000
10,000
15,000
20,000
BB'
360
340
320
300
280
260
240
0
5,000
10,000
15,000
CC'
400
380
360
340
320
300
0
5,000
10,000
15,000
Legend
Caldera
Elevation
upper sea level (m)
-50 - 150
150 - 300
300 - 450
450 - 600
600 - 750
750 - 900
900 - 1150
1150 - 1400
1400 - 1850
1850 - 2600
Ongatiti Formation
A
A'
B
B'
C
C'
N
0
10 Km

Figure 2

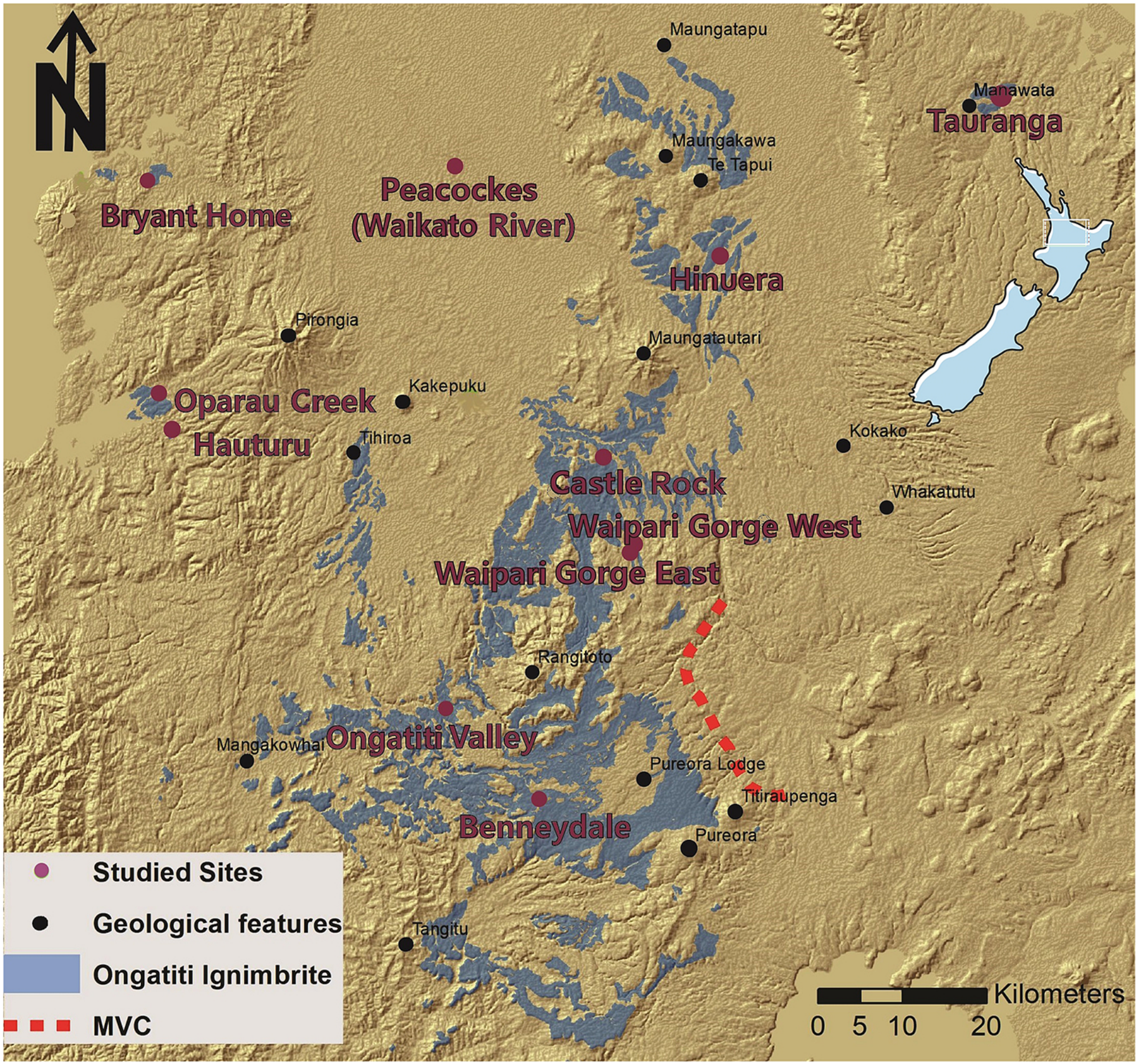
Maungatapu
Manawata
Tauranga
Maungakawa
Te Tapui
Peacockes
(Waikato River)
Bryant Home
Hinuera
Pirongia
Maungatautari
Kakepuku
Oparau Creek
Hauturu
Tihiroa
Kokako
Castle Rock
Whakatutu
Waipari Gorge West
Waipari Gorge East
Rangitoto
Ongatiti Valley
Mangakowhai
Pureora Lodge
Titiraupenga
Benneydale
Pureora
Tangitu
Studied Sites
Geological features
Ongatiti Ignimbrite
MVC
Kilometers
0 5 10 20

Figure 3

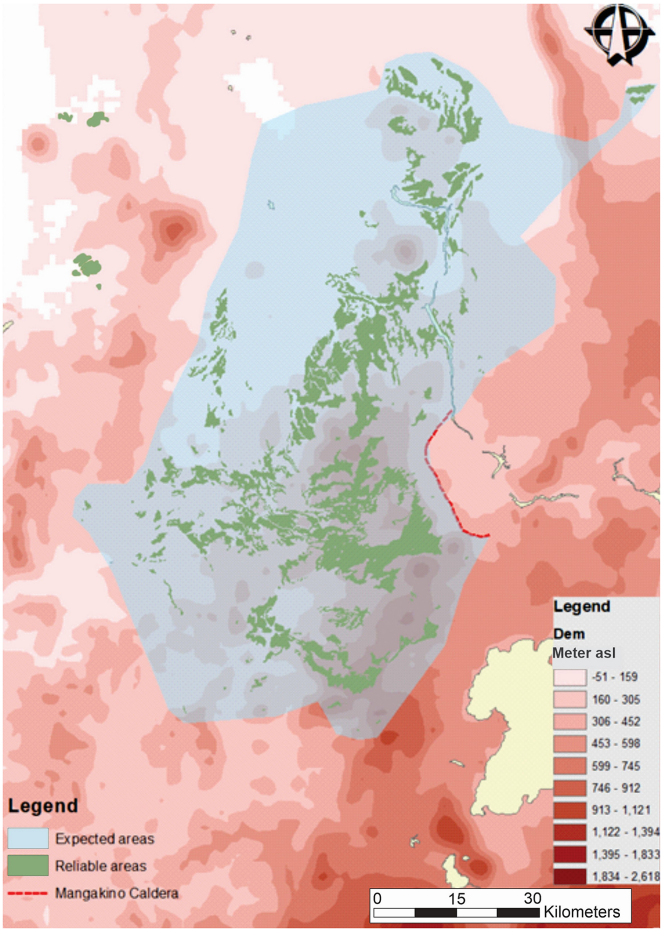
Legend
Dem
Meter asl
-51 - 159
160 - 305
306 - 452
453 - 598
599 - 745
746 - 912
913 - 1,121
1,122 - 1,394
1,395 - 1,833
1,834 - 2,618
Legend
Expected areas
Reliable areas
Mangakino Caldera
0
15
30
Kilometers

Figure 4

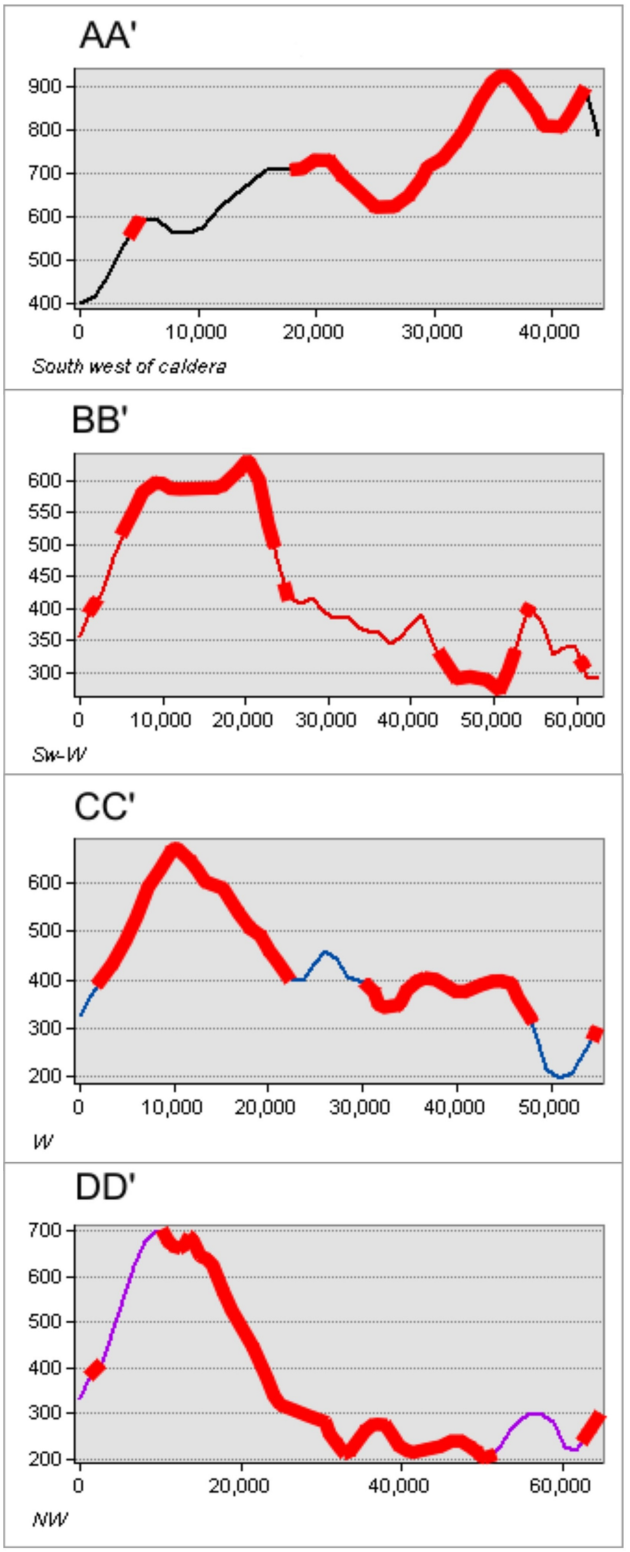
AA'
900
800
700
600
500
400
0
10,000
20,000
30,000
40,000
South west of caldera
BB'
600
550
500
450
400
350
300
0
10,000
20,000
30,000
40,000
50,000
60,000
Sw-W
CC'
600
500
400
300
200
0
10,000
20,000
30,000
40,000
50,000
W
DD'
700
600
500
400
300
200
0
20,000
40,000
60,000
NW

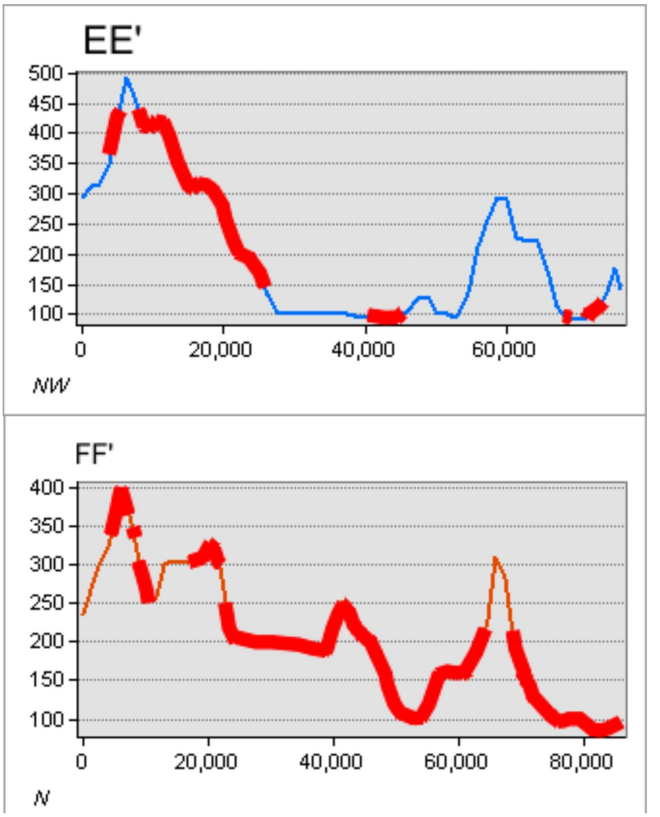
EE'
500
450
400
350
300
250
200
150
100
0
20,000
40,000
60,000
NW
FF'
400
350
300
250
200
150
100
0
20,000
40,000
60,000
80,000
N

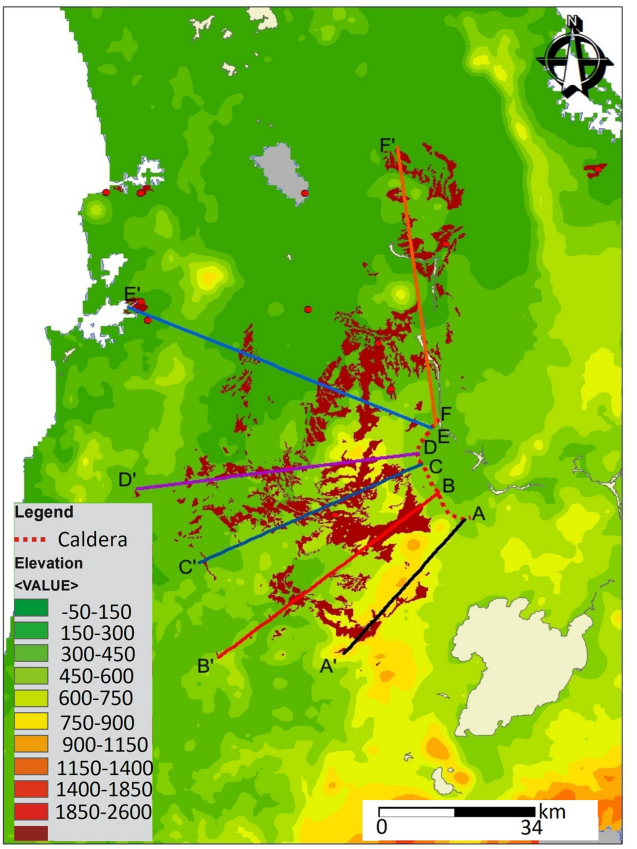
N
F'
E'
F
E
D
C
B
A
D'
C'
B'
A'
Legend
Caldera
Elevation
<VALUE>
-50-150
150-300
300-450
450-600
600-750
750-900
900-1150
1150-1400
1400-1850
1850-2600
0
34
km

Figure 5

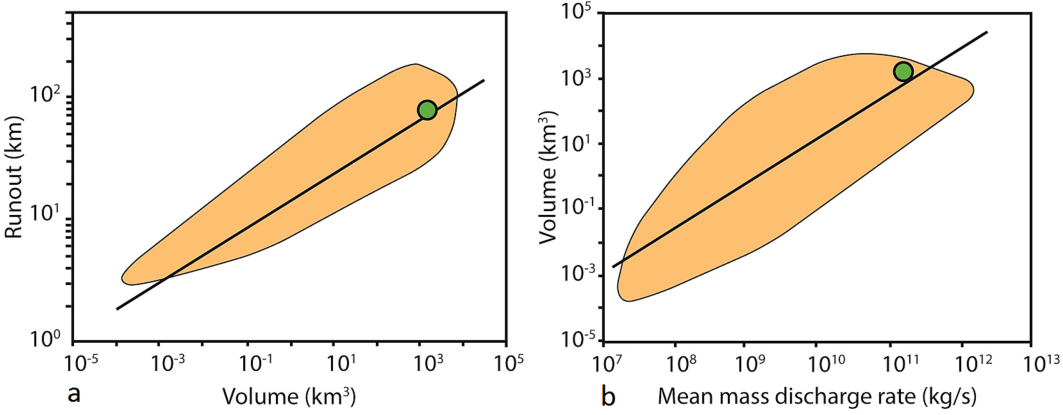
Runout (km)
10^2
10^1
10^0
10^{-5}
10^{-3}
10^{-1}
10^1
10^3
10^5
a
Volume (km³)
Volume (km³)
10^5
10^3
10^1
10^{-1}
10^{-3}
10^{-5}
10^7
10^8
10^9
10^{10}
10^{11}
10^{12}
10^{13}
b
Mean mass discharge rate (kg/s)

Figure 6

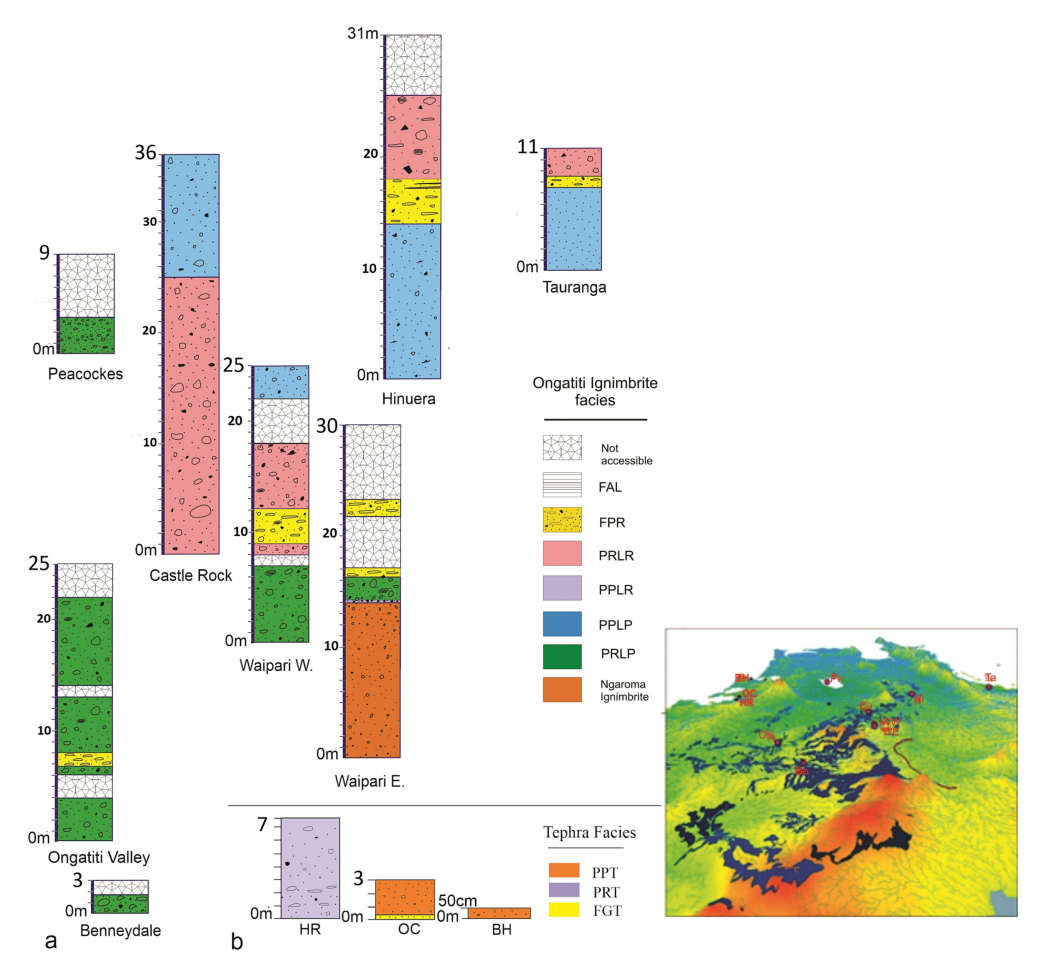
31m
20
10
0m
Hinuera
11
0m
Tauranga
36
30
20
10
0m
Castle Rock
9
0m
Peacockes
25
20
10
0m
Waipari W.
30
20
10
0m
Waipari E.
25
20
10
0m
Ongatiti Valley
3
0m
Benneydale
a
7
0m
HR
3
0m
OC
50cm
0m
BH
b
Ongatiti Ignimbrite facies
Not accessible
FAL
FPR
PRLR
PPLR
PPLP
PRLP
Ngaroma Ignimbrite
Tephra Facies
PPT
PRT
FGT

Figure 7

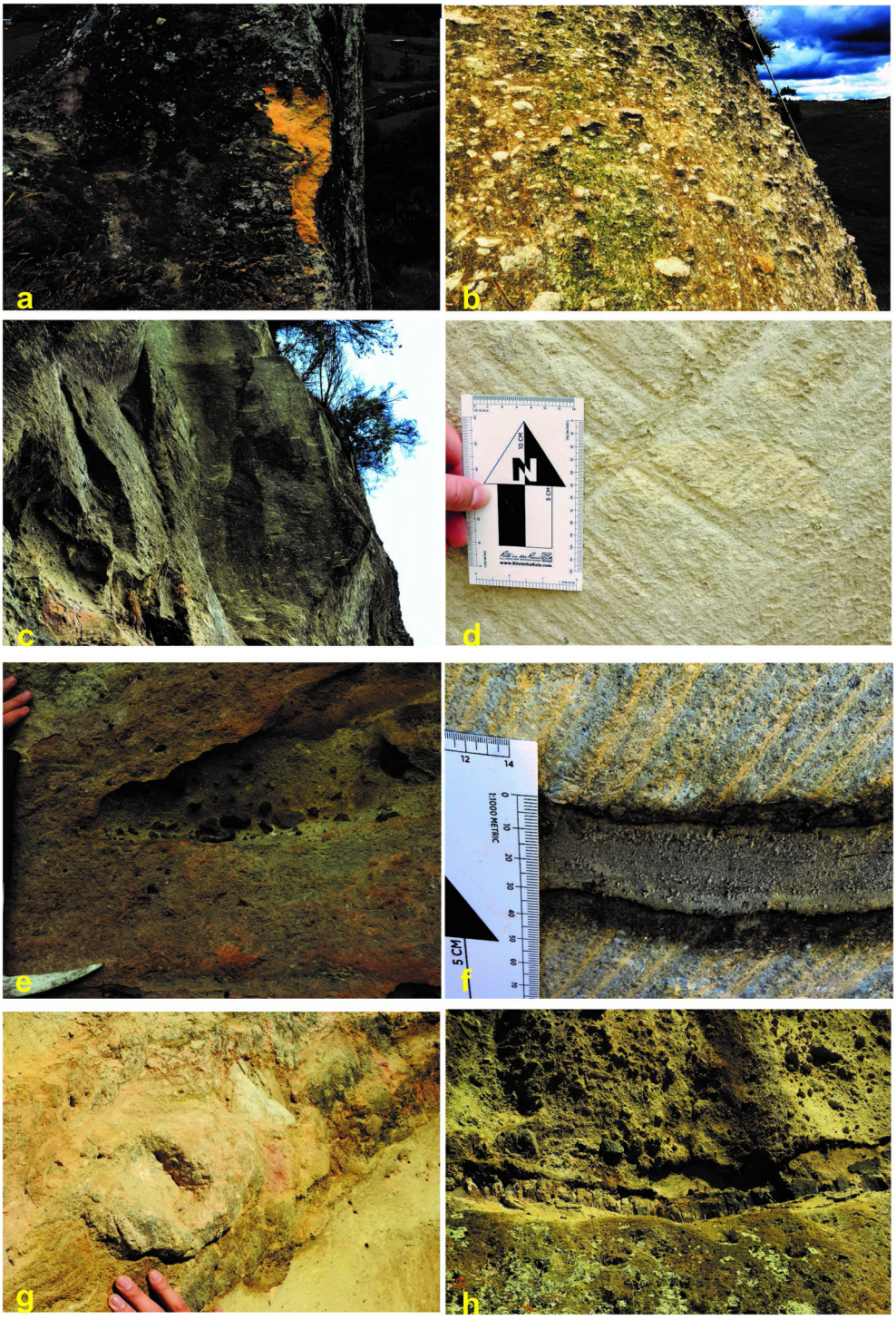

Figure 8

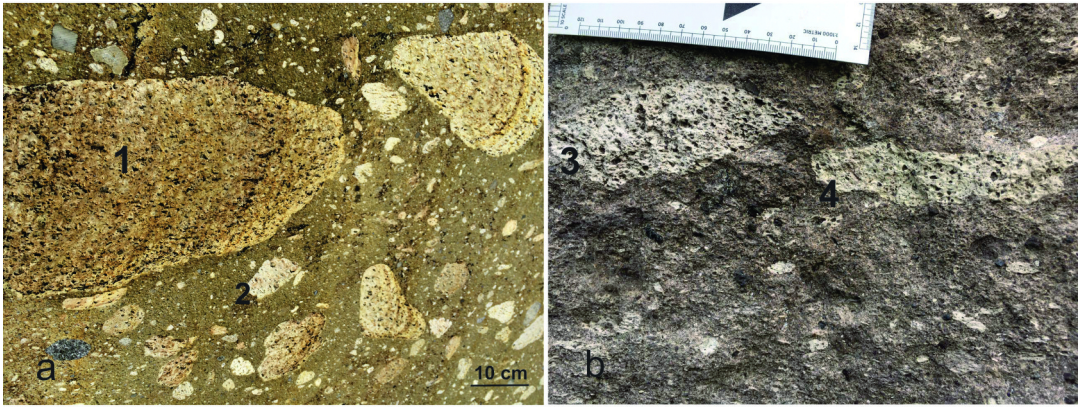

Figure 9

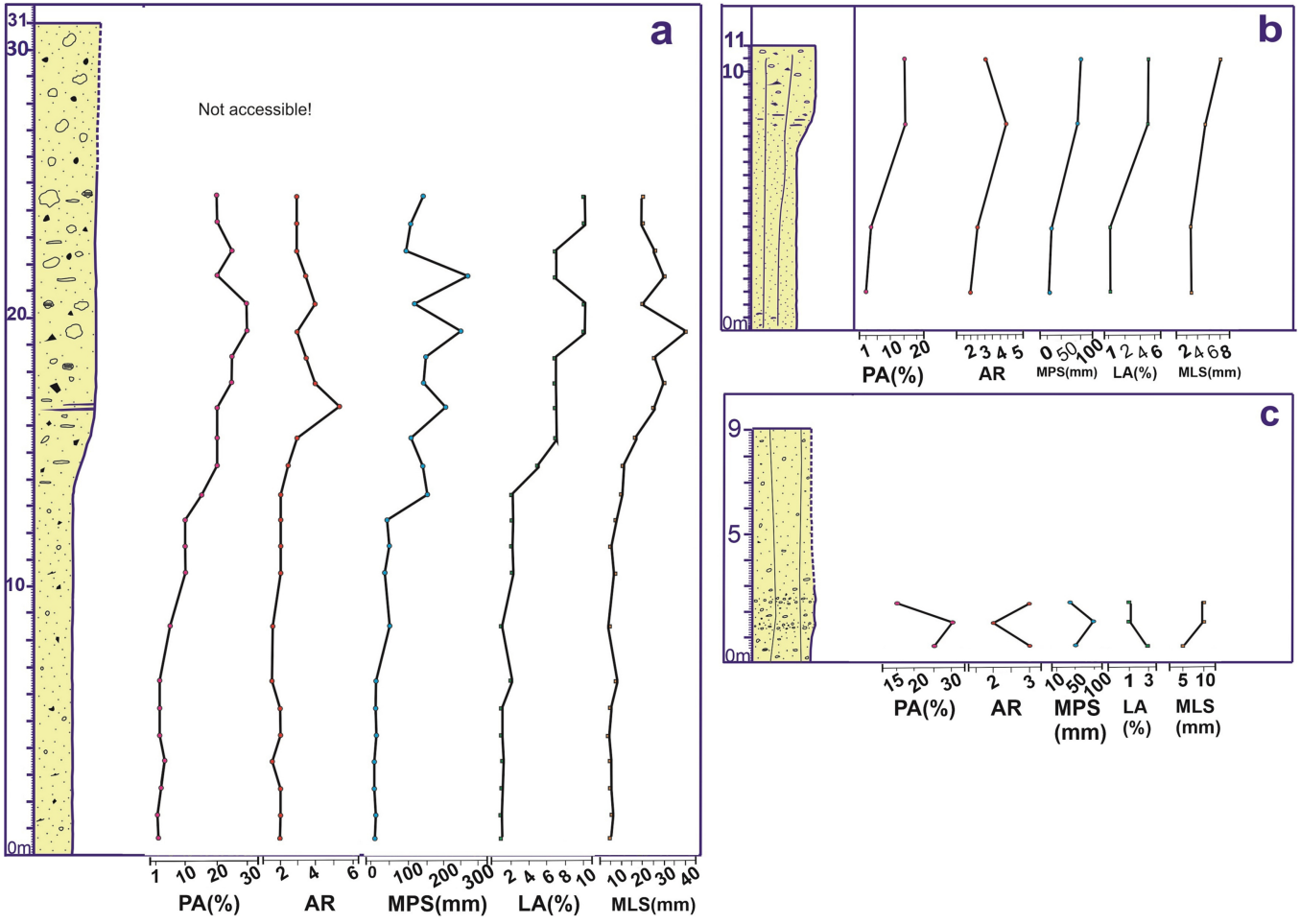
a
Not accessible!
31
30
20
10
0m
1 10 20 30
PA(%)
2 4 6
AR
0 100 200 300
MPS(mm)
2 4 6 8 10
LA(%)
10 20 30 40
MLS(mm)
b
11
10
0m
1 10 20
PA(%)
2 3 4 5
AR
0 50 100
MPS(mm)
1 2 4 6
LA(%)
2 4 6 8
MLS(mm)
c
9
5
0m
15 20 30
PA(%)
2 3
AR
10 50 100
MPS (mm)
1 3
LA (%)
5 10
MLS (mm)

Figure 10A

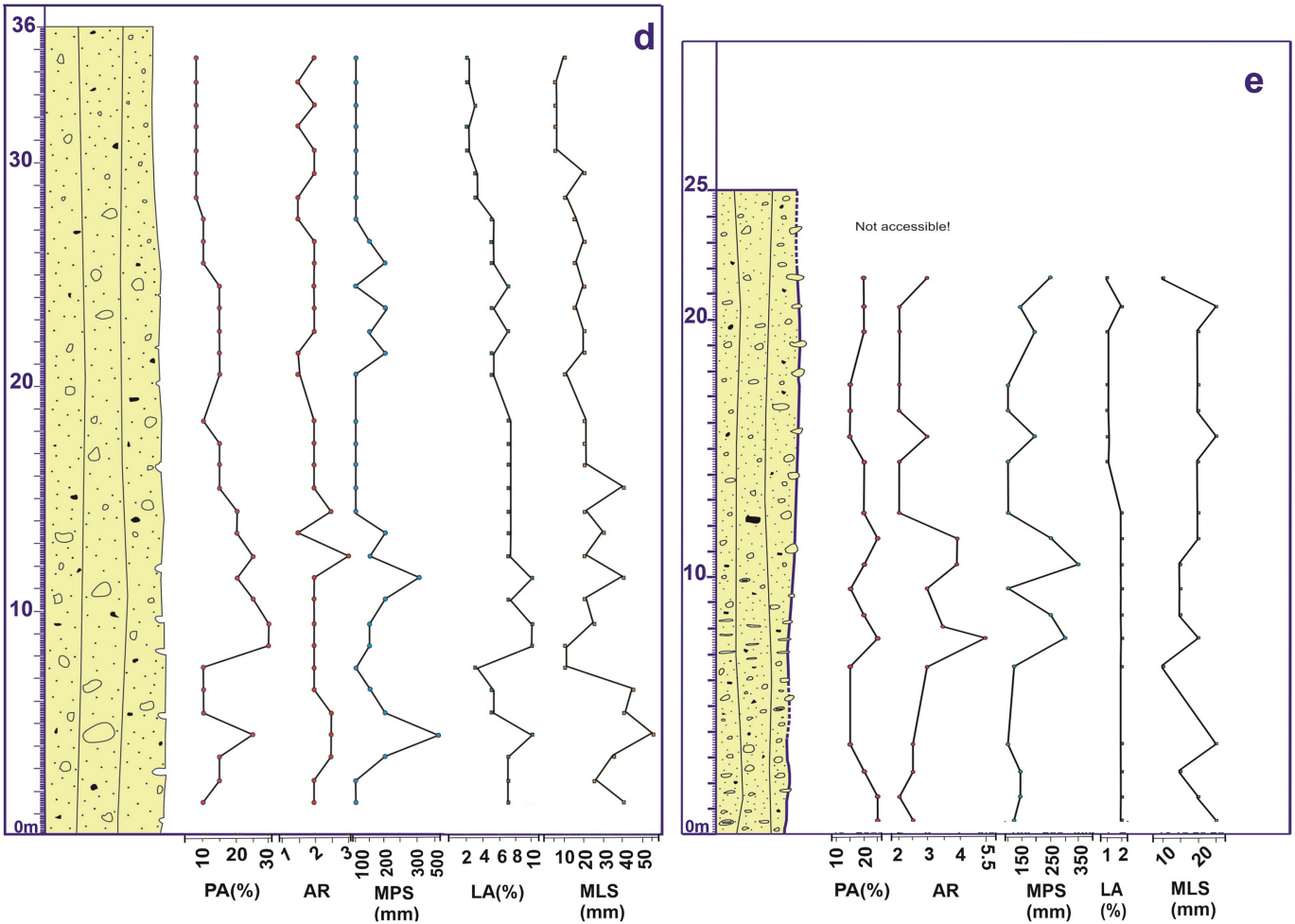
d
36
30
20
10
0m
PA(%)
AR
MPS (mm)
LA(%)
MLS (mm)
e
25
20
10
0m
Not accessible!
PA(%)
AR
MPS (mm)
LA (%)
MLS (mm)

Figure 10B

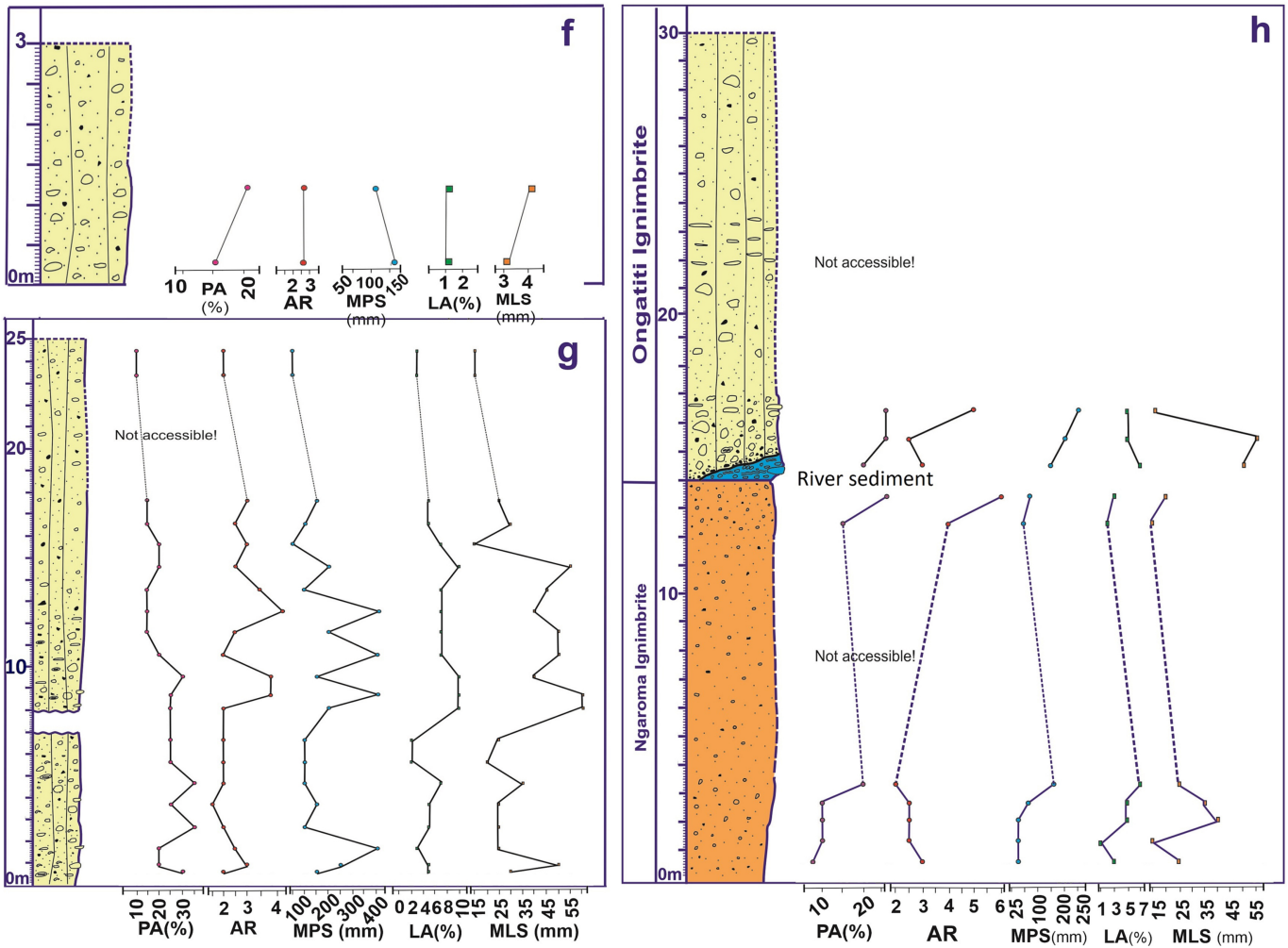
f
3
0m
10 PA (%) 20
2 3 AR
50 100 150 MPS (mm)
1 2 LA(%)
3 4 MLS (mm)
g
25
20
10
0m
Not accessible!
10 20 30 PA(%)
2 3 4 AR
100 200 300 400 MPS (mm)
0 2 4 6 8 10 LA(%)
10 15 25 35 45 55 MLS (mm)
h
30
20
10
0m
Ongatiti Ignimbrite
Ngaroma Ignimbrite
Not accessible!
River sediment
Not accessible!
10 20 PA(%)
2 3 4 5 6 AR
25 100 200 250 MPS(mm)
1 3 5 7 LA(%)
15 25 35 45 55 MLS (mm)

Figure 10C

Figure 11

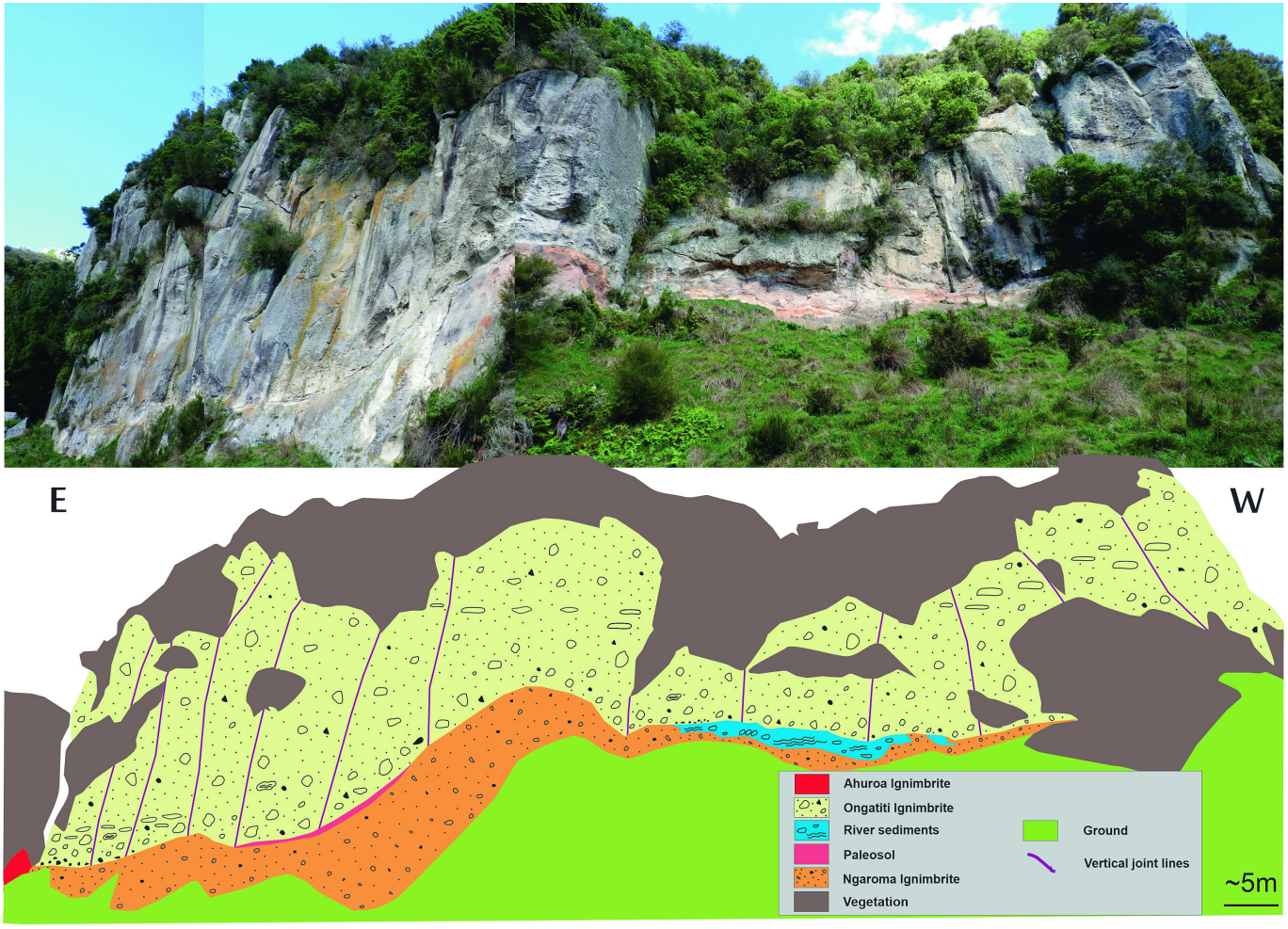
E
W
Ahuroa Ignimbrite
Ongatiti Ignimbrite
River sediments
Paleosol
Ngaroma Ignimbrite
Vegetation
Ground
Vertical joint lines
~5m

Figure 12

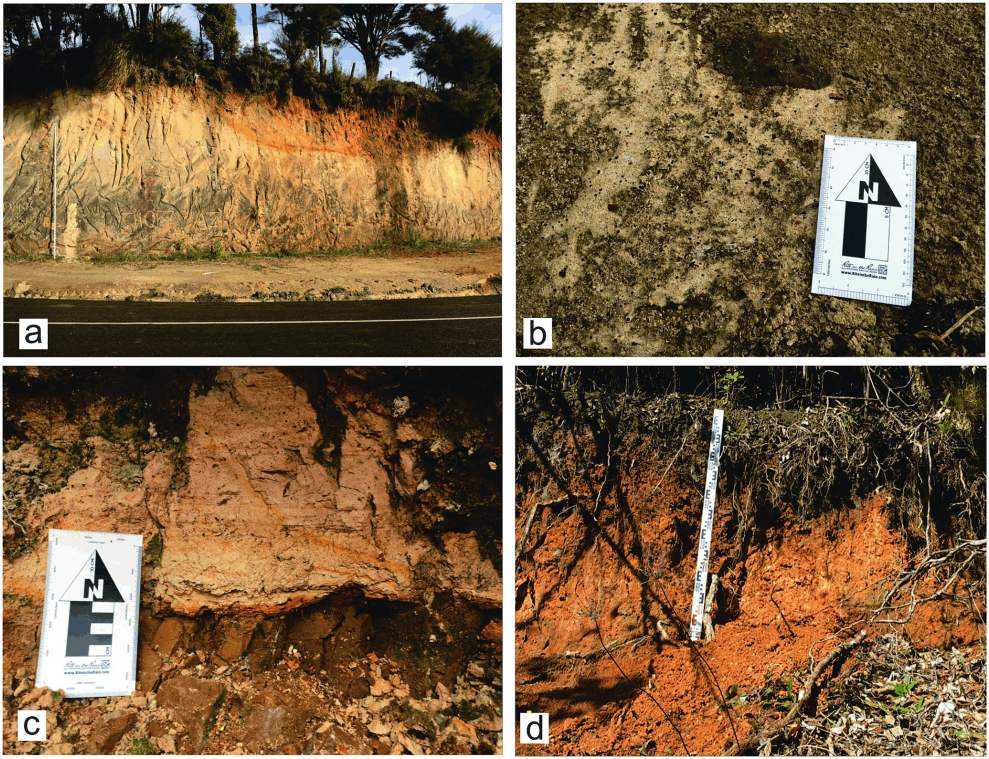

Figure 13

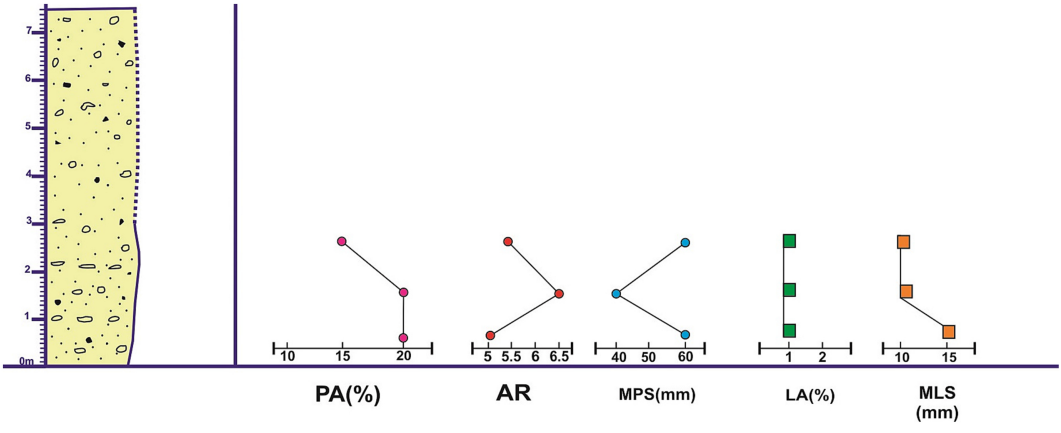

Figure 14

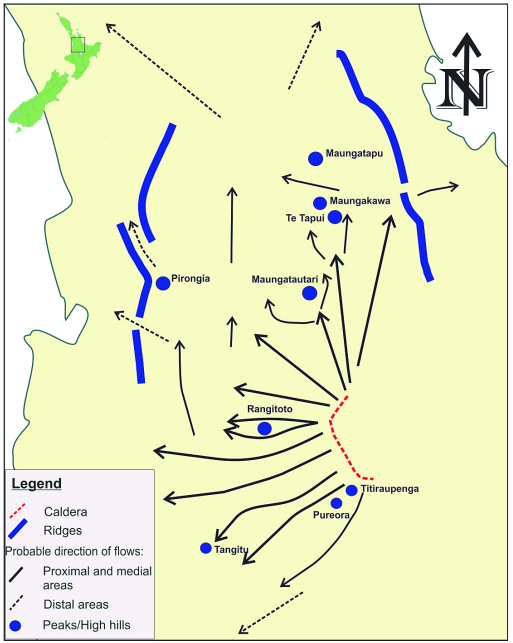
Maungatapu
Maungakawa
Te Tapui
Pirongia
Maungatautari
Rangitoto
Titiraupenga
Pureora
Tangiru
Legend
Caldera
Ridges
Probable direction of flows:
Proximal and medial areas
Distal areas
Peaks/High hills

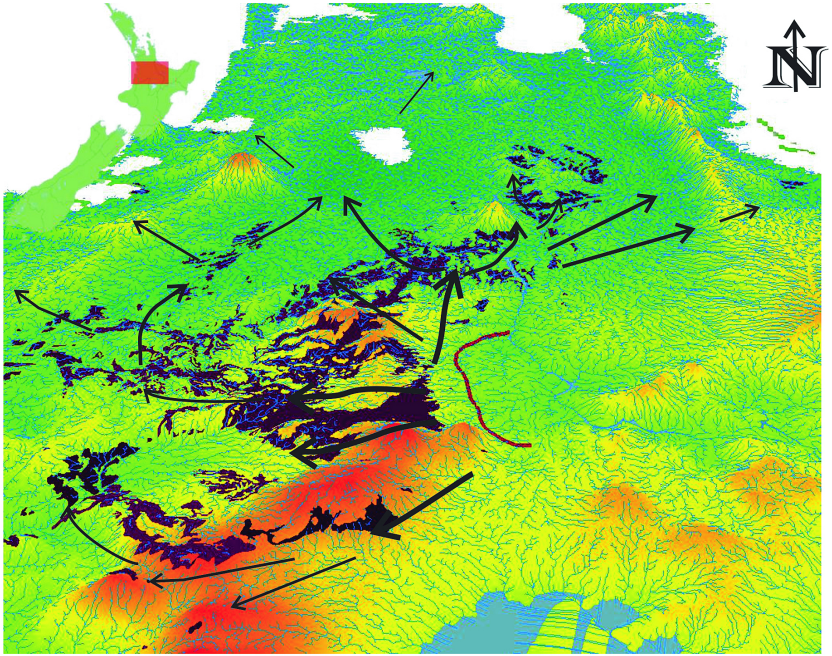

Figure 15

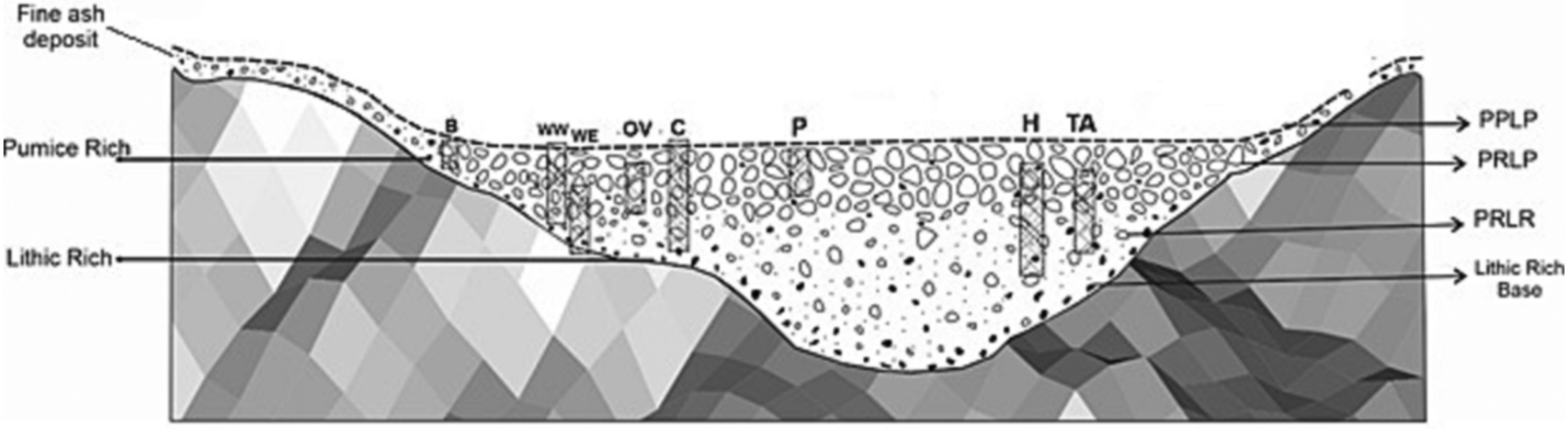
Fine ash deposit
Pumice Rich
Lithic Rich
B
WW
WE
OV
C
P
H
TA
PPLP
PRLP
PRLR
Lithic Rich Base

Figure 16